https://doi.org/10.5194/egusphere-2026-4788
Preprint. Discussion started: 13 August 2026

Impact of the chemical regime on highly oxygenated molecule and secondary organic aerosol formation: Effects of varying the importance of NO, $HO_2\cdot$, $RO_2\cdot$ reactions on α-pinene photooxidation products

Yarê Baker[1,a], Veronica Geretti[2], Sungah Kang[1], Rongrong Wu[1,b], Hui Wang[1], Quanfu He[1,c], Thorsten Hohaus[1], Annika Zanders[1], Mathias Bachner[3], Cheng Wu[2], Thomas J. Bannan[4], Simon P. O'Meara[4,5], Aristeidis Voliotis[4], Mattias Hallquist[2], Gordon McFiggans[4,☆], Sören R. Zorn[1], and Thomas F. Mentel[1,☆]

[1]Institute of Energy and Climate Systems, ICE-3, Forschungszentrum Jülich GmbH, 52425, Jülich, Germany
[2]Department of Chemistry and Molecular Biology, University of Gothenburg, 41390 Gothenburg, Sweden
[3]Institute of Technology and Engineering, ITE, Forschungszentrum Jülich GmbH, 52425, Jülich, Germany
[4]Department for Earth and Environmental Sciences, University of Manchester, Manchester, M13 9PL, UK
[5]National Centre for Atmospheric Science, University of Manchester, Manchester, M13 9PL, UK
[a]present address: Atmospheric Chemistry Department, Leibniz Institute for Tropospheric Research, 04318 Leipzig, Germany
[b]present address: Department for Earth and Environmental Sciences, University of Manchester, Manchester, M13 9PL, UK
[c]present address: Earth, Ocean and Atmospheric Sciences (EOAS) Thrust, Function Hub, The Hong Kong University of Science and Technology, 511458 Guangzhou, China
☆retired

Correspondence to: Yarê Baker (yare.baker@alumni.fh-aachen.de) and Sören R. Zorn (s.zorn@fz-juelich.de)

Abstract. An important source of secondary organic aerosol (SOA) are highly oxygenated molecules (HOMs) formed by atmospheric oxidation of volatile organic compounds. HOM formation is governed by the fate of HOM peroxy radicals ($RO_2\cdot$) which depends on the availability of reaction partners ($RO_2\cdot$, $HO_2\cdot$, NO) and on their overall lifetime - factors often insufficiently explored in laboratory studies.

We performed α-pinene photooxidation experiments systematically exploring these parameters and present the impacts on HOM and SOA formation within a generic framework explaining the changes in HOM production. Steady-state experiments were performed in the SAPHIR-STAR atmospheric simulation chamber. The reaction regime was shifted by increasing $HO_2\cdot$ and NO, separately and simultaneously, while keeping the α-pinene primary oxidation conditions constant. $(NH_4)_2SO_4$ particles were added to observe gas-phase HOM condensation and investigate product volatilities.

We find decreasing SOA formation potential when moving away from $RO_2\cdot$-dominated regimes. One reason is the suppression of HOM accretion product formation from HOM-$RO_2\cdot$+$RO_2\cdot$. Alkoxy radicals ($RO\cdot$) from $RO_2\cdot$+$RO_2\cdot$ or $RO_2\cdot$+NO play another important role. $RO\cdot$ are crucial intermediates in certain HOM formation pathways but also produce lower-mass, more fragmented HOM with higher volatility, decreasing SOA formation potential. Additionally, $RO_2\cdot$+NO forms organic nitrates, which we show have higher volatility than other termination products. Our mechanistic considerations illustrate which factors

https://doi.org/10.5194/egusphere-2026-4788
Preprint. Discussion started: 13 August 2026

impact the HOM product distribution and explain the reduced SOA formation through changes in HOM composition and volatility.

1. Introduction

Secondary organic aerosol (SOA) is an important constituent of atmospheric aerosol with global models estimating annual production rates of 16 to 121 Tg a^{-1} (Tsigaridis et al., 2014). One important source of SOA are highly oxygenated molecules (HOMs) produced by the atmospheric oxidation of volatile organic compounds (VOCs).

Autoxidation is a key process in HOM formation. It allows for reaching the high degree of oxidation necessary for the partitioning of oxidation products into the particle phase. During the autoxidation, after the initial attack of an oxidant, O_2 attaches to the radical site forming a peroxy radical ($RO_2\cdot$), which quickly undergoes an intramolecular H-shift forming a hydroperoxide group and reforming a reactive radical that can undergo another autoxidation step. This mechanism leads to the fast formation of HOMs with high oxygen numbers and high O/C ratios (Ehn et al., 2014; Crounse et al., 2013).

Each time a peroxy radical is formed during the autoxidation chain there are multiple possible reaction pathways. The intramolecular H-shift described above continues the autoxidation chain, but different termination reactions are also possible. Bimolecular termination reactions with NO, $HO_2\cdot$ and other $RO_2\cdot$ are the main termination pathways in the atmosphere. Intramolecular termination is another possibility. Therefore, the reactivity related to the composition of the atmosphere in terms of $RO_2\cdot$, $HO_2\cdot$ and NO determines if and which HOMs are formed from autoxidation.

The complexity and variability of the atmosphere cannot easily be simulated in laboratory studies, for example due to the simple fact that higher than atmospheric VOC concentrations must be applied because of instrumental detection limits. In recent years this led not only to an increased awareness and reevaluation of atmospheric simulation chamber experiment results, but also to efforts to better characterize and design such experiments, see for example Kenagy et al. (2024) and Yang et al. (2025). In experiments focusing on understanding HOM formation pathways a common concern is the overemphasis of $RO_2\cdot$+$RO_2\cdot$ reactions. $RO_2\cdot$ cross reactions form accretion products, which due to their low volatility may lead to an overestimation of SOA yields (Schervish and Donahue, 2021). Furthermore, depending on the $RO_2\cdot$+$RO_2\cdot$ reaction rate coefficients the overall amount of formed HOMs may decrease due to interruptions of the autoxidation chain in more competitive surroundings, i.e., mixtures with higher reactivity due to either availability of termination reactions with faster reaction rate coefficients and/or higher availability of reaction partners.

In this study we present a set of experiments systematically varying the importance of HOM-$RO_2\cdot$ reactions with $HO_2\cdot$, NO and other $RO_2\cdot$, as well as varying the overall reaction rate of bimolecular reactions in competition to autoxidation on the example of the α-pinene photooxidation system.

For the analysis, we introduce a characterization of the chemical reaction regime based on two general concepts: 1) The speed of bimolecular reactions, which also determines the size of the chemical sink, as defined by the pseudo-first order reaction rate

https://doi.org/10.5194/egusphere-2026-4788
Preprint. Discussion started: 13 August 2026

sum of $HO_2\cdot$, NO, and $RO_2\cdot$ in competition to the ongoing autoxidation. And 2) the composition of this HOM-$RO_2\cdot$ sink as percentages of reactions with $HO_2\cdot$, NO, and $RO_2\cdot$.

This characterization relies on the application of generic reaction rate coefficients and cannot capture individual reaction pathways. However, our results demonstrate that such a simplified scheme can still be used to understand the changes in concentration and product distribution of HOMs in different chemical regimes. In our experiments we have also utilized targeted seeding, which allows direct conclusions on how changes in the gas-phase product composition affect the SOA formation potential of the system.

While this work presents the whole framework of experiments and analysis, its focus is on the influence of NO. The results focusing on the effects of $HO_2\cdot$ have been previously published in Baker et al. (2024). In the anthropogenic atmosphere, NO is a ubiquitously important trace gas, even in rural or remote areas (for measured examples see Peng et al. (2019)). This ubiquity makes understanding the influence of NO in chemical regimes that are otherwise defined by biogenic influences especially interesting.

2. Method

2.1. Generic chemistry scheme

The expected α-pinene+$\cdot$OH reaction pathways have been described in detail in our previous publication describing the system with high $HO_2\cdot$ (Baker et al., 2024). Therefore, here only the key points are introduced before moving on to the expected reaction pathways of $RO_2\cdot$+NO.

The key species in the autoxidation of α-pinene are peroxy radicals with the sum formulas $C_{10}H_{15}O_x\cdot$ and $C_{10}H_{17}O_x\cdot$. The hydrogen number depends on the initial radical formation step. The oxygen number increases in steps of two with increasing number of autoxidation steps. The autoxidation is rapid and H-shift rates of about 0.01 – 0.1 s^{-1} and faster have been reported (Piletic and Kleindienst, 2022; Berndt, 2021; Xu et al., 2019; Vereecken et al., 2007). The H-shift rate is dependent on the relative position of the hydrogen to the peroxy group and the surrounding functional groups (Otkjaer et al., 2018; Vereecken and Nozière, 2020). The autoxidation chain will run until all available H-shift reactions are slower than the competing termination reactions or no H-shifts are available.

The termination reactions discussed here are the bimolecular reactions with NO, $HO_2\cdot$ and other $RO_2\cdot$, as well as internal termination. The scheme of a possible internal termination reaction that was discussed for cyclohexene by Rissanen et al. (2014) is shown in Supplement **Fig. S1**. The result of such a reaction is the elimination of $\cdot$OH and the formation of a carbonyl termination group, leading to $C_{10}H_{n-1}O_{x-1}$ in comparison to the precursor peroxy radical.

From now on the notations of "carbonyl", "hydroperoxide", etc. always refer to the functional group formed in the termination reaction of the $RO_2\cdot$. Furthermore, we use the term "family" for groups of oxidation products that only differ in the number of oxygens, but have the same number of carbon, hydrogen, and nitrogen atoms.

https://doi.org/10.5194/egusphere-2026-4788
Preprint. Discussion started: 13 August 2026

The main expected products of RO_2·+HO_2· termination are hydroperoxides (RO_2·+HO_2· → ROOH + O_2). The reaction of RO_2·+RO_2· has three possible termination pathways. Firstly, the formation of an alcohol and a carbonyl: RO_2·+R'O_2·→R-OH + R'=O + O_2. As for the termination forming a hydroperoxide with HO_2·, the number of carbon atoms is the same as that of the VOC precursor, therefore such HOM products are referred to as monomers (HOM-Mon).

Secondly, RO_2·+RO_2· can lead to accretion product formation in the simplest case by RO_2·+R'O_2·→R-O-O-R'+O_2 besides other mechanisms leading to accretion products with less C-atoms than in the precursor VOC (Peräkylä et al., 2023; Franzon et al., 2024). This HOM accretion product class (HOM-Acc) has a higher number of carbon atoms than the VOC precursor, and due to the high molecular weights and large number of oxygen atoms HOM-Acc are expected to be of extremely low volatility. In the case of the reaction of a "larger" (higher oxidation degree, higher molar mass) HOM-RO_2· with a "smaller" less oxidized RO_2· the accretion product formation will increase the SOA yield, as the small RO_2· is scavenged into the particle phase. For HOM-RO_2· it is expected that both a HOM-Mon or a HOM-Acc product would be of such low volatility that it contributes to SOA formation (Pullinen et al., 2020; McFiggans et al., 2019).

The third possible RO_2·+RO_2· reaction is the formation of alkoxy radicals (RO_2·+R'O_2·→RO·+R'O·+O_2). Kang et al. (2025) showed recently the role of isomerization of HOM-RO· in HOM formation. The reactions of alkoxy radicals are described in **Sect. 2.1.1.**

In systems containing NO_x (NO+NO_2) a new class of products is formed: organic nitrates (ON). For HOM-RO_2· in general, the reaction with NO is the major expected reaction pathway as only acyl peroxy radicals (RC(=O)O_2·) form stable products in reactions with NO_2. ON formed by reaction of other peroxy radicals with NO_2 are often thermally unstable and decompose back into the reactants. The RO_2·+NO_2 reaction leads to the formation of peroxyacetyl nitrates (PAN-like organic compounds) (Seinfeld and Pandis, 2016). For PAN compounds formed in α-pinene oxidation Noziere and Barnes (1998) reported dissociation rates similar to PAN itself.

The reaction of RO_2·+NO has two possible pathways: The formation of an alkoxy radical (RO_2·+NO→RO·+NO_2) or the formation of an ON (RO_2·+NO→$RONO_2$). If an ON is formed, NO is added to the molecule without the loss of any group. Therefore, in comparison to the termination with HO_2· or RO_2· the termination with NO results in products of higher mass and O/C ratio. ON formed from $C_{10}H_{15}O_x$· will have the molecular formula of $C_{10}H_{15}NO_{x+1}$, while ON formed from $C_{10}H_{17}O_x$· will have the molecular formula of $C_{10}H_{17}NO_{x+1}$. Thus, ON can be uniquely related to one of the precursor radical families.

The branching ratio of RO_2·+NO to the formation of an ON (termination) or the formation of an alkoxy radical depends on the size and substitution of the RO_2·, as well as on pressure and temperature. The alkoxy radical formation is normally the expected major reaction pathway (Ziemann and Atkinson, 2012). The "master chemical mechanism" (MCM v3.3.1) (Jenkin et al., 1997; Saunders et al., 2003) adopted a branching ratio of about 0.7 into alkoxy radical formation for a-pinene derived RO_2·. Kang et al. (2025) determined a similar ratio of 0.64 for HOM-RO_2·. Unlike HO_2·, NO is thus expected to directly influence the oxidation chain, while HO_2· is mainly expected to determine the termination group. However, it should be noted that the reaction with HO_2· can in limited cases facilitate alkoxy radical formation (RO_2·+HO_2·→RO·+·OH+O_2) (Jenkin et al., 2019).

https://doi.org/10.5194/egusphere-2026-4788
Preprint. Discussion started: 13 August 2026

Furthermore, the NO_x and HO_x ($\cdot OH+HO_2\cdot$) cycles interact via the reaction of $HO_2\cdot$ and NO ($HO_2\cdot + NO \rightarrow \cdot OH + NO_2$), and at high NO_2 concentrations via the reaction of $\cdot OH$ and NO_2 forming HNO_3 (Seinfeld and Pandis, 2016). These interactions lead to a nonlinear effect of NO_x on HOM formation, as discussed by Nie et al. (2023). Overall, the interactions of HOM-$RO_2\cdot$ with NO_x are complex and further depend on the NO/NO_2 ratio.

2.1.1. Reactions of alkoxy radicals

Alkoxy radicals are highly reactive species with three major reaction pathways: $RO\cdot$ can react with O_2 forming a carbonyl and $HO_2\cdot$. However, this reaction is only important for small, less functionalized alkoxy radicals, and for HOM-$RO\cdot$ the reaction with O_2 is too slow to compete with the other reaction pathways.

The second reaction pathway is an α-bond scission, which results in two molecules: an alkyl radical and a closed-shell molecule containing a carbonyl group. The alkyl radical can reform a $RO_2\cdot$ radical, which may continue the autoxidation chain. We refer to such scission reactions as "fragmentation" as it leads to formation of products with less carbon atoms than the VOC precursors (HOM-Frag products). Due to the lower molar mass and higher volatility of such fragments they are less likely to contribute to SOA formation.

The third reaction pathway is an intramolecular H-shift as shown in **Fig. 1**. This isomerization reaction will form an alcohol from the alkoxy group and an alkyl radical. The alkyl radical then adds O_2 to reform a $RO_2\cdot$, and the whole process is called an alkoxy-peroxy step (Vereecken and Peeters, 2010).

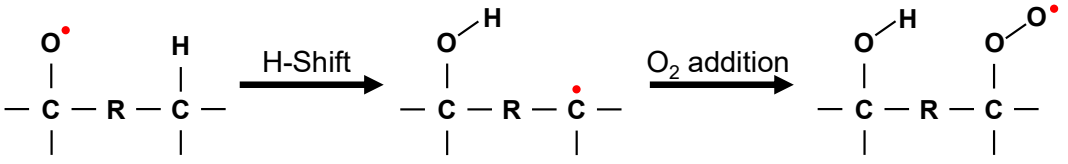

Figure 1 Reaction scheme of alkoxy-peroxy step

H-shifts retaining the carbon backbone become more likely with increasing functionality of the alkoxy radical (Vereecken et al., 2007). The formed $RO_2\cdot$ can again continue the autoxidation chain, as reported by Nie et al. (2023) and Mentel et al. (2015). Kang et al. (2025) recently reported that circa 50 % of alkoxy radicals formed in α-pinene+$\cdot OH$ systems undergo isomerization, so that inclusion of alkoxy-peroxy steps can lead to an extension of the autoxidation chain length and thus lead to HOMs with higher oxidation degrees. Next to peroxy radicals, alkoxy radicals are the second important radical species in the HOM formation mechanism. Especially in systems with NO, alkoxy radicals play a major role due to their fast formation from $RO_2\cdot$+NO.

2.2. Categorization of the chemical regime

In this work we use a generic framework to categorize the chemical reaction regime for (HOM-)$RO_2\cdot$ based upon two mechanistical aspects:

https://doi.org/10.5194/egusphere-2026-4788
Preprint. Discussion started: 13 August 2026

1) The expected sum over the bimolecular pseudo first order reaction rates representing the competition with ongoing autoxidation (reflecting the HOM-RO_2· lifetime with respect to bimolecular termination in competition to lifetime with respect to autoxidation).
2) The expected contributions of RO_2·, HO_2·, and NO to the bimolecular RO_2· reaction pool.
These two metrics are essential to understand HOM-RO_2· chemistry and its impact on SOA formation. The framework is based on the box modeling for the gas-phase chemistry (see **Sec. 3.3**) and generic reaction rate coefficients for the reactions of RO_2· with RO_2·, HO_2·, and NO. The applied generic reaction rate coefficients can be found in **Tab. 1** and were chosen in accordance with MCM v3.3.1 (Jenkin et al., 1997; Saunders et al., 2003) and Roldin et al. (2019).

Table 1 Overview of applied generic reaction rate coefficients $k_{Reaction}$ for bimolecular HOM-RO_2· reactions

Reaction	Equation	Resulting reaction rate coefficient (T= 293.15 K)	Reference
HOM-RO_2·+NO	$2.70 \cdot 10^{-12} \cdot \exp(\frac{360}{T})$	$9.2 \cdot 10^{-12}$ $cm^3 \cdot s^{-1}$	MCM v3.3.1 (Jenkin et al., 1997; Saunders et al., 2003)
HOM-RO_2·+HO_2·	$2.91 \cdot 10^{-13} \cdot \exp(\frac{1300}{T})$	$24.5 \cdot 10^{-12}$ $cm^3 \cdot s^{-1}$	MCM v3.3.1 (Jenkin et al., 1997; Saunders et al., 2003))
HOM-RO_2·+R'O_2·	-	$5.0 \cdot 10^{-12}$ $cm^3 \cdot s^{-1}$	Roldin et al. (2019)

For our discussions we use the in the laboratory relatively easy to achieve "simple" RO_2·+RO_2· dominated case as the reference point, utilizing the framework to understand and explain the observed shifts in the HOM product distribution between the different chemical regimes.
This comparison method was introduced in Baker et al. (2024) and is possible due to the constant turnover of α-pinene+·OH. The turnover is calculated as $k_{OH} \cdot [\alpha\text{-pinene}]_{SS} \cdot [OH]_{SS}$, utilizing the steady-state (SS) concentrations of the reaction partners and a reaction rate coefficient of $k_{OH} = 5.36 \cdot 10^{-11}$ $cm^3 s^{-1}$ (Atkinson and Arey, 2003). However, to further account for small variations in the turnover due to experimental imperfections a normalization with the calculated turnover was applied for all comparisons.
A constant turnover is important to avoid effects of oxidant scavenging (McFiggans et al., 2019) and to assure comparability between the different chemical regimes: The entry channel into the α-pinene photooxidation was kept constant, so that the production of first-generation RO_2· was constant. Thus, the different chemical reaction regimes only shifted the reaction pathways of RO_2· produced in the oxidation.

2.2.1. Estimation of RO_2· bimolecular reaction rate in competition to ongoing autoxidation

The bimolecular reaction rate S_{RO_2} is calculated as shown in **Eq. (1)** and the calculation results in a pseudo-first order reaction rate (unit: s^{-1}). The calculation applies the generic reaction rate coefficients from **Tab. 1** as well as the box-modeled steady-state concentrations of the reaction partners. The concentration of RO_2· is calculated as the sum of the concentrations of all RO_2· species in the MCM v3.3.1 (Jenkin et al., 1997; Saunders et al., 2003).

https://doi.org/10.5194/egusphere-2026-4788
Preprint. Discussion started: 13 August 2026

$$S_{RO_2} = k_{\mathrm{RO_2+NO}} \cdot [NO]_{SS} + k_{\mathrm{RO_2+HO_2}} \cdot [HO_2]_{SS} + k_{\mathrm{RO_2+RO_2}} \cdot [RO_2]_{SS} \quad \textbf{(1)}$$

The bimolecular termination represented by S_{RO_2} is in competition with the ongoing autoxidation (and wall loss) of the RO₂·. As a benchmark, we chose a reaction rate coefficient of $k_{autox.} = 0.1\ s^{-1}$ for the ongoing autoxidation of HOM-RO₂· derived from a-pinene+·OH. This value is chosen in accordance with values reported in the literature (Piletic and Kleindienst, 2022; Berndt, 2021; Xu et al., 2019; Vereecken et al., 2007), but of course omits the large variety of individual autoxidation reaction rate coefficients. However, we expect autoxidation steps with reaction rate coefficients close to $k_{autox.}$ and faster to be significant contributors in the autoxidation chain leading to HOM-RO₂· formation.

Therefore, if the termination reaction rate can compete with such autoxidation rates, an earlier termination of the autoxidation is expected. Products with a lower degree of oxidation and thus higher volatility will be formed, and the fast termination will reduce the overall amount of observed HOMs and SOA.

2.2.2. RO₂· reaction partner contribution to bimolecular reaction rate

The termination pathways with NO, HO₂·, RO₂· lead to different closed-shell products, as explained in **Sec. 2.1**. Certain functional groups correlate with the importance of one reaction partner. Carbonyls are products of RO₂·+RO₂· (or internal termination), ON can only be formed in the RO₂·+NO reaction, and more fragmentation is expected in systems with NO due to the increased importance of alkoxy radical formation (**Sec. 2.1.1**). Hydroperoxide formation is expected to dominate in systems with high HO₂·, and all systems shifting away from RO₂·+RO₂· will reduce the importance of accretion product formation from RO₂·+RO₂·. Especially the formation of less HOM-Acc or more fragmentation products is expected to decrease the SOA formation potential. Furthermore, the volatility of the HOM can be influenced by the specific functional group formed in the termination, further affecting the SOA formation potential.

The calculation of the contribution of one reaction partner uses the same variables as the calculation of the total bimolecular sink size and is calculated as shown in **Eq. (2)**.

$$contribution\ reactant = \frac{k_{\mathrm{RO_2+reactant}} * [reactant]_{SS}}{S_{RO_2}} \quad \textbf{(2)}$$

3. Experimental methods

3.1. Chamber set-up and experimental conditions

All experiments were performed as steady-state experiments in the continuously stirred tank reactor SAPHIR-STAR at the Forschungszentrum Jülich. The detailed chamber, measurement, and experiment set-up for this measurement campaign were described in Baker et al. (2024). The SAPHIR-STAR reactor is a borosilicate glass cylinder with a volume of 2000 L. The

https://doi.org/10.5194/egusphere-2026-4788
Preprint. Discussion started: 13 August 2026

inflow during the experiments was 32 L min^{-1}, resulting in a residence time of circa 60 minutes. The temperature was 20 °C and the relative humidity 50 % in all experiments.

·OH was produced via ozone photolysis and the subsequent reaction of $O(^1D)$ with water vapor. Photolysis was achieved with two UV-C lamps (wavelength 254 nm) mounted in quartz cylinders in the middle of the chamber oriented perpendicular to the cylinder axis. In all experiment phases ·OH was the dominant sink of a-pinene (compared to O_3) with α-pinene+·OH accounting for ≥ 75 % of the α-pinene turnover.

An important feature of SAPHIR-STAR is the movable shielding surrounding the lamps. The shielding can be set to cover a defined percentage of the lamp and was used to adjust the ·OH production in the chamber after changes in the chemical regime. Considering all experiments and experiment phases this led to photolysis frequencies of $j(O^1D)$ ranging from $0.8 \cdot 10^{-3}$ s^{-1} to $2.6 \cdot 10^{-3}$ s^{-1}. Additionally, the ozone inflow was adjusted to keep the ·OH concentration approximately constant across all chemical regimes.

The ·OH concentration was calculated from the decay of α-pinene as described by Kiendler-Scharr et al. (2009). The applied reaction rate coefficients were $k_{OH} = 5.36 \cdot 10^{-11}$ $cm^3 s^{-1}$ (Atkinson and Arey, 2003) for the α-pinene+·OH reaction and $k_{O_3} = 9.25 \cdot 10^{-17}$ $cm^3 s^{-1}$ for the α-pinene+O_3 reaction, both at 20 °C.

In experiments with NO addition, a set of UV-A lamps (wavelength 365 nm) was utilized to photolyze NO_2 to NO and O_3. The UV-A lamps were turned on during all experiment phases including background measurements to assure no additional change in the system upon NO addition due to the UV-A light turning on (due to heat or photolysis). The $j(NO_2)$ photolysis frequency was experimentally determined as $1.0 \cdot 10^{-3}$ s^{-1}. It should be mentioned that this is lower than typical atmospheric values, for example, Cho et al. (2023) measured $j(NO_2)$ during summer in Germany and reported values of around $4.0 \cdot 10^{-3}$ s^{-1}.

For NO addition experiments two series of experiments were performed. In the first series only NO was added, while in the second series both the concentrations of NO_x and HO_2· were increased. The HO_2· concentration was increased via the addition of CO and the subsequent reaction of CO + ·OH + O_2 → CO_2 + HO_2·. The ·OH concentration was kept stable by the adjustments of the lamp opening and the O_3 concentration as described above (for details on the experimental method see Baker et al. (2024)).

3.2. Instrument set-up

A large suite of instruments was used to measure gas and particle phase. A cavity ring down spectrometer (G2401 Cavity Ringdown Spectrometer, Picarro Inc.) was applied to measure CO_2, CO, CH_4 and H_2O. O_3 was measured with a UV-photometer (O342e, Envea GmbH). The VOC precursor concentration was measured via proton-transfer-reaction mass spectrometry (PTR-TOF-MS; Ionicon GmbH).

NO and NO_x were measured by chemiluminescence (nCLD899, Eco Physics GmbH coupled to a home-built photolytic converter). However, due to a drift in measurement signal, data in two experiments needed further correction (for details see

https://doi.org/10.5194/egusphere-2026-4788
Preprint. Discussion started: 13 August 2026

Supplement **Sec. S2**). In each steady state VOC, O_3, and NO/NO_x sampling was switched between inlet and outlet of the chamber to provide input concentrations as well as steady-state concentrations of the reactants.

To measure the particle number concentration a condensation particle counter (CPC, Model 3788, TSI GmbH) was used, while a scanning mobility particle sizer (SMPS; Model 3080, TSI GmbH) with a CPC (Model 3788, TSI GmbH) provided information about the particle size distribution. A high-resolution aerosol mass spectrometer (HR-TOF AMS; Aerodyne Inc.) was used to measure the aerosol composition.

The main instrument for detection of the oxidized product species was a chemical ionization mass spectrometer (CIMS). We utilized a multi-scheme ionization (MION, Karsa Oy) inlet CIMS coupled to a long TOF (LTOF, Tofwerk AG, resolution ~8500 for peaks at >200 m/Q). For more information on the MION inlet see Rissanen et al. (2019). As the MION allows switching between different reagent ion chemistries, bromide and nitrate were used as the reagent ions in this study (inlet flow 10 L min^{-1}, resulting in inlet reaction times of 60 ms for bromide and 600 ms for nitrate). The bromide mode was used for detection of the $HO_2\cdot$ radical and lesser oxidized products (Albrecht et al., 2019; Sanchez et al., 2016).

The nitrate mode was used for the detection of closed shell HOMs, and HOM-$RO_2\cdot$. However, in experiments with organic nitrate formation not all HOM-$RO_2\cdot$ that were detectable in the pure $RO_2\cdot$, $HO_2\cdot$ regimes could be assigned due to two factors. Firstly, ON-HOM compounds can have similar (odd) molar masses to certain HOM-$RO_2\cdot$, leading to overlapping peaks. Furthermore, the fast reaction of specific HOM-$RO_2\cdot$ with NO decreased their steady-state concentrations, making the clear identification of a small shoulder on a larger ON-HOM peak difficult (for details see Supplement **Sec. S4**).

Bianchi et al. (2017) suggested using the terminology of HOM only for compounds with six or more oxygen. However, as we are interested in the shift of the product's oxidation degree between different regimes, we also included a few products with four and five oxygen. The identified compounds for each regime are listed in Supplement **Sec. S3**.

3.3. Modeling set-up

A zero-dimensional box model applying the chemistry represented in the MCM v3.3.1 (Jenkin et al., 1997; Saunders et al., 2003) was utilized for experiment planning and evaluation. The model was set up using the boundary conditions of the SAPHIR-STAR chamber with constant input of temperature, relative humidity, chamber inflows, inflow concentrations of α−pinene, O_3, NO, and CO, as well as the lamp status of the UV-C and UV-A lamps. Photolysis frequencies in the model were scaled to match $J(O^1D)$ and $J(NO_2)$ determined in chamber characterization experiments, and the lamps were numerically switched on/off. A scaling factor representing the uncovered percentage of the lamp was additionally implemented for the UV−C light. Differential equations were solved using FACSIMILE within the institute software package EASY (EASY Version 5.69b). More details on the model set-up can be found in the Supplement of Baker et al. (2024).

The model calculations were able to reproduce the concentrations observed for α-pinene, O_3, CO, NO_2, and ·OH within the experimental uncertainties. Somewhat larger discrepancies were observed for NO due to the low steady-state concentrations (<1 parts per billion by volume (ppbv)), however, there were no absolute discrepancies larger than 0.2 ppbv.

https://doi.org/10.5194/egusphere-2026-4788
Preprint. Discussion started: 13 August 2026

The box model is a crucial tool for our analysis framework as it provides the necessary input on the expected $HO_2\cdot$ and $RO_2\cdot$ sum concentrations. However, since no direct measurements of these concentrations are available, larger uncertainties apply. The modeled $HO_2\cdot$ and $RO_2\cdot$ sum concentrations and further details on the model set-up can be found in the Supplement **Sec. S5**.

4. Results and Discussion

For the analysis of the effects of NO and $HO_2\cdot$ availability on HOM and SOA formation we utilize a framework to characterize the chemical regime based on two parameters: The overall bimolecular reaction rate for $RO_2\cdot$ and the expected contribution of $HO_2\cdot$, NO, and $RO_2\cdot$ to this reaction rate. These parameters were determined using generic rate coefficients (see **Sec. 2.2**) and box model results for the concentrations of the reaction partners.

As explained in **Sec. 3.1** two different experiment series were performed. In the experiments for the "NO system" only NO was added, while in the experiments for the "mixed system" NO was added, and the concentration of $HO_2\cdot$ was increased. For an overview of all performed steady states see Supplement **Tab. S5**. For the visualization of the effects, we focus on four cases: Two in the NO system and two in the mixed system with both increased NO and $HO_2\cdot$. The characteristics within our framework of these four cases as well as of the high $HO_2\cdot$ and base case are shown in **Fig. 2**. **Figure 2a)** visualizes the chemical regime of each case in a triangular plot in a similar manner to Peng et al. (2019).

In the NO system a "middle NO" case ($[NO]_{SS}$= 0.2 ppbv) was chosen where 70 % of $RO_2\cdot$ were expected to be terminated with NO. The remaining 30 % were equally divided between $RO_2\cdot+HO_2\cdot$ and $RO_2\cdot+RO_2\cdot$. At the high NO level ($[NO]_{SS}$ = 0.5 ppbv), the reaction of $RO_2\cdot$+NO was expected to dominate 95 % of the termination reactions (see **Fig. 2 a)**).

The total bimolecular reaction rate was calculated as 0.06 s^{-1} for the middle NO case and as 0.17 s^{-1} for the high NO case (see **Fig. 2 b)**). With the assumption of an average autoxidation rate of 0.1 s^{-1} at middle NO the bimolecular reaction rate was still expected to be slower than many autoxidation rates, while at high NO the pseudo-first order reaction rate of $k_{RO2+NO}\cdot[NO]$ was faster than the average expected autoxidation rate. However, the model results and assumed reaction rate coefficients cannot describe the system fully and have high uncertainties. Moreover, as shown by Kang et al. (2025), HOM alkoxy radicals can continue the autoxidation chain via an alkoxy-peroxy step, meaning that a part of the bimolecular NO and $RO_2\cdot$ reactions do not lead to termination of the autoxidation chain.

For the mixed case with high $HO_2\cdot$ and NO for the lower NO addition ($[NO]_{SS}$= 0.2 ppbv), the overall pseudo-first order reaction rate coefficient was 0.09 s^{-1}, which is close to the utilized generic average autoxidation rate of 0.1 s^{-1}. Thus, it can be expected that the chemical termination reduces the amount of observed autoxidation products. This middle NO, high $HO_2\cdot$ case is especially interesting because the contribution to the chemical sink by $RO_2\cdot+HO_2\cdot$ and $RO_2\cdot$+NO was expected to be about equal (approximately 50 % by $RO_2\cdot+HO_2\cdot$ and 45 % by $RO_2\cdot$+NO, with the remaining 5 % by $RO_2\cdot+RO_2\cdot$). Note that reaction of HOM-$RO_2\cdot$ with $HO_2\cdot$ is expected to only result in HOM-RO in specific constellations (Iyer et al., 2018; Eddingsaas et al., 2012; Hasson et al., 2005; Jenkin et al., 2019). Therefore, alkoxy radical formation is expected to be suppressed by $HO_2\cdot$.

https://doi.org/10.5194/egusphere-2026-4788
Preprint. Discussion started: 13 August 2026

In the high NO, high $HO_2\cdot$ case ($[NO]_{SS}$= 0.4 ppbv), the termination was expected to be dominated by $RO_2\cdot$+NO (80 %), with $HO_2\cdot$ contributing around 18 %. The total bimolecular reaction rate was expected to be significantly larger with a pseudo-first order rate coefficient around 0.17 s^{-1}. These calculations and comparisons of generic reaction rate coefficients only serve as trend indicators.

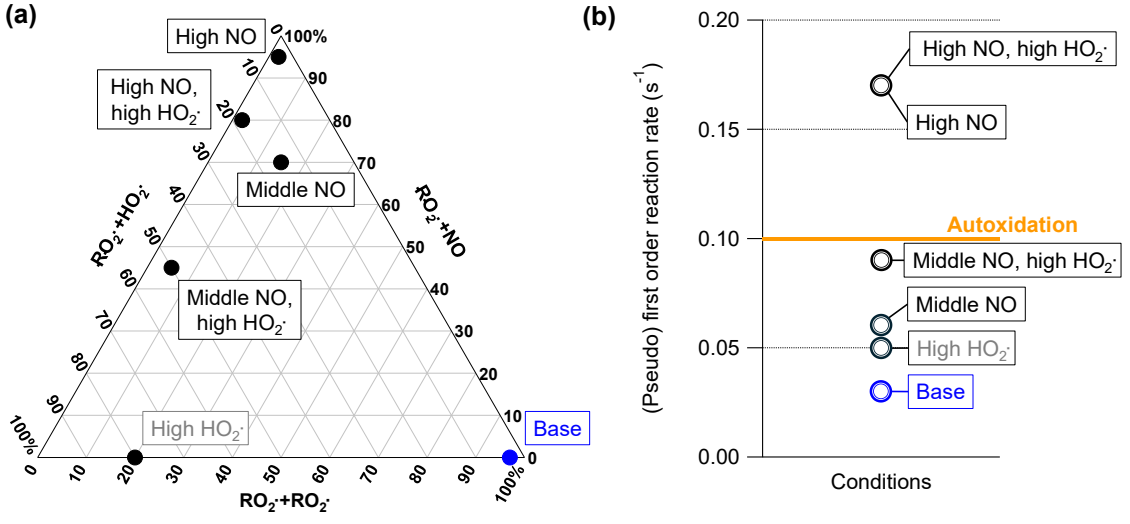

Figure 2 Classification of the chemical regimes covered by the experiments: a) Triangle plot showing the distribution between bimolecular reactions for $RO_2\cdot$ with NO, $HO_2\cdot$ and $RO_2\cdot$. Which grid lines correspond to which axes are indicated by the inclination of the axes' labels. b) (Pseudo) first order bimolecular reaction rate in comparison to average autoxidation rate.

4.1. Termination product contributions as proof of utility for the chemical regime framework

The generic framework introduced above describes the reaction pathways expected for HOM-$RO_2\cdot$. To demonstrate the value of the framework, we can compare the HOM families representing the termination pathways measured under different conditions to the expected contribution of a reaction partner (NO, $HO_2\cdot$, $RO_2\cdot$) as shown in **Fig. 2a**). In the following we will present two cases showing the evolution of both products from NO and $HO_2\cdot$ in the different chemical regimes.

The termination of $RO_2\cdot$+NO leads to formation of ON-HOM with the dominant source of ON in our system being $RO_2\cdot$+NO. Another possible ON source is the reaction of acyl peroxy radicals with NO_2 forming PAN-like compounds. Though we cannot fully exclude this reaction pathway we checked the importance of PAN-like ON-HOM and found their influence to be minor. For this investigation the UV-A light was turned off during one experiment at middle NO concentrations. With the UV-A light off the concentration of NO decreased while the importance of NO_2 increased. In steady state this led to a decrease in NO concentration of about 40 %, while the sum of all detected ON compounds decreased by 30 %. The similar decrease in NO and ON indicates that indeed the major source of ON-HOM in our system was $RO_2\cdot$+NO reactions, though the slightly smaller decrease in ON-HOM indicates some formation from $RO_2\cdot$+NO_2.

https://doi.org/10.5194/egusphere-2026-4788
Preprint. Discussion started: 13 August 2026

The formation of ON-HOM was observed in two product classes: HOM-Mon and HOM-Frag. Within the HOM-Mon class a few observed ON-HOM contained two nitrogen atoms, however, their contribution was minor (for more details see Supplement **Sec. S7**). For an overview of all identified ON see the peaklist in Supplement **Tab. S2** and **Tab. S3**.

To characterize the contribution of the ON-HOM to the overall product sum for different contributions of RO_2·+NO to the termination reactions, we utilized three different NO levels for both the NO system and the mixed system (see Supplement **Tab. S5** for an overview of framework parameters).

In the NO system's high NO case a contribution of RO_2·+NO of close to 100 % was realized, and thus no further significant increase in contribution of ON products is possible at a given branching ratio between ON and alkoxy radical formation. Indeed, assuming a given branching ratio into ON formation, the ON contribution should increase linearly with increasing contribution of RO_2·+NO termination to the chemical sink.

In **Fig. 3** the contribution of the ON-HOM to the overall product sum is plotted against the calculated RO_2·+NO contribution to the bimolecular RO_2· reactions. The RO_2·+NO contribution serves only as a guideline as it is based on the application of generic reaction rate coefficients. The uncertainty is further increased as there were no HO_2· or RO_2· measurements to verify the modeled $[RO_2\cdot]_{SS}$ sum and $[HO_2\cdot]_{SS}$ concentrations. Despite these caveats **Fig. 3** shows a good linear trend supporting the merit of the simple estimations by our framework.

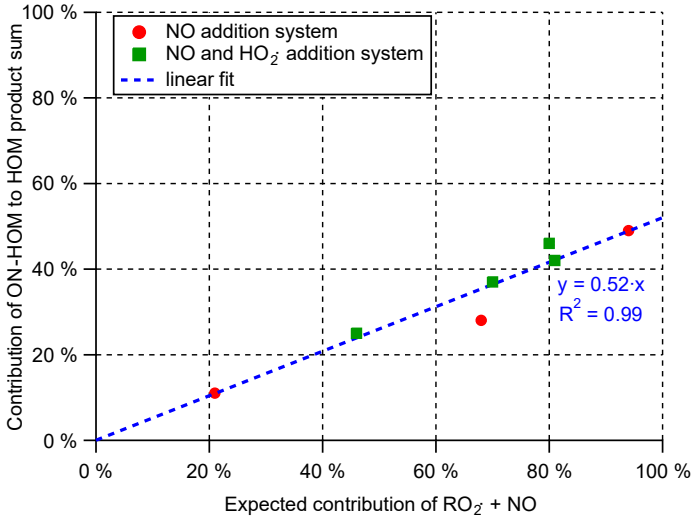

Figure 3 Contribution of measured ON-HOM product sum to overall product HOM sum as a function of the RO_2·+NO contribution to the overall RO_2· bimolecular reaction rate. Linear trend (blue dotted line) is forced through zero.

Furthermore, the results for both the mixed system with available HO_2· and the pure NO system fall on the same line. For the high NO case where the termination was dominated by the reaction with NO, ON-HOM contributed around 50 % of all observed HOM. Our results compare well to Pullinen et al. (2020), who reported a contribution of ON-HOM of about 50 % to the total observed HOM sum for α-pinene photooxidation under high NO_x conditions. We observed a higher contribution of ON than the assumed branching ratios of ON formation from RO_2·+NO of 0.3 utilized in the MCM v3.3.1 (Jenkin et al., 1997;

https://doi.org/10.5194/egusphere-2026-4788
Preprint. Discussion started: 13 August 2026

Saunders et al., 2003)). However, this is to be expected as the other 0.7 branch into alkoxy formation. Alkoxy radicals can continue the autoxidation chain by performing a so-called alkoxy-peroxy step, reforming a peroxy radical. For plausibility let us consider the three first reaction cycles forming $RO_2\cdot$ and let us assume according to Kang et al. (2025) that 50 % of HOM-RO· undergo an alkoxy-peroxy step forming HOM-$RO_2\cdot$ and thus continue the reaction chain. Let us also apply a 0.3 branching ratio into ON formation as utilized in the MCM v3.3.1 (Jenkin et al., 1997; Saunders et al., 2003)). A visualization of the calculation can be found in Supplement **Fig. S3**. After these three cycles, 45 % of the original HOM-$RO_2\cdot$ have terminated as an ON, while only 4 % are still continuing the reaction. This simple consideration agrees well with our observations in chemical regimes where $RO_2\cdot$+NO is expected to be the dominant termination pathway.

A correspondent comparison for the termination products of $RO_2\cdot+HO_2\cdot$ is somewhat more complicated since there is no well-defined product class which can only be assigned to $RO_2\cdot+HO_2\cdot$. The best option is to look at the fraction of $C_{10}H_{18}O_z$ since they can only arise from $C_{10}H_{17}O_x\cdot$ radicals. $C_{10}H_{18}O_z$ are the expected hydroperoxide termination products from $C_{10}H_{17}O_x\cdot+HO_2\cdot$, with the other distinct $C_{10}H_{17}O_x\cdot$ products being $C_{10}H_{17}NO_z$-ON. However, $C_{10}H_{18}O_z$ can also be the alcohol termination product from $C_{10}H_{17}O_x\cdot+RO_2\cdot$, so that the fraction of $C_{10}H_{18}O_z$ is only an unambiguous indicator for the importance of $RO_2\cdot+HO_2\cdot$ in systems where the $RO_2\cdot+RO_2\cdot$ termination is negligible. Additionally, systems without significant contribution of $RO_2\cdot$+NO cannot be utilized for the comparison, as here $C_{10}H_{18}O_z$ is the only product that can be clearly attributed to $C_{10}H_{17}O_x\cdot$. This approach is superior to other potential options that utilize or additionally utilize the $RO_2\cdot+HO_2\cdot$ termination products of $C_{10}H_{15}O_x\cdot$, as $C_{10}H_{16}O_z$ cannot only also be the alcohol termination product of $C_{10}H_{15}O_x\cdot+RO_2\cdot$, but also the carbonyl product from $C_{10}H_{17}O_x\cdot+RO_2\cdot$ or internal termination of $C_{10}H_{17}O_x\cdot$. The fraction of $C_{10}H_{18}O_z$ of clear $C_{10}H_{17}O_x\cdot$ products is therefore used as the best available indicator for the contribution of $RO_2\cdot+HO_2\cdot$ to the bimolecular termination sink under the following boundaries: a) Contribution of $RO_2\cdot+RO_2\cdot$ to the termination sink ≤5 % and b) availability of NO as a termination partner. **Figure 4** shows the available data which obey these constraints.

https://doi.org/10.5194/egusphere-2026-4788
Preprint. Discussion started: 13 August 2026

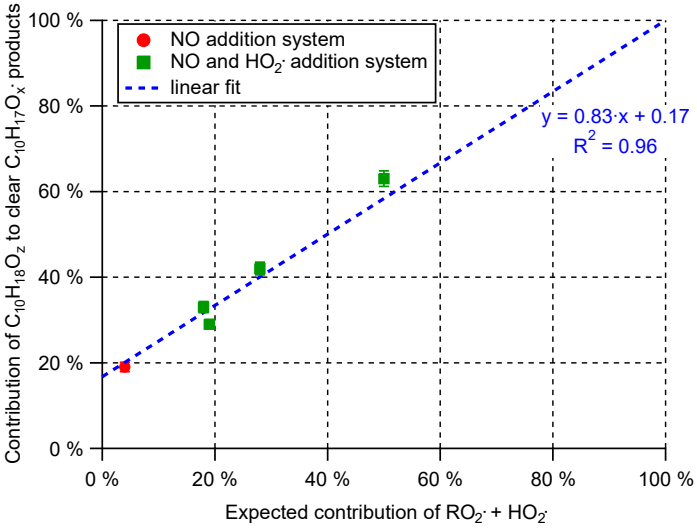

Figure 4 Contribution of measured $C_{10}H_{18}O_z$ product sum to unambiguous $C_{10}H_{17}O_x$· product sum ($C_{10}H_{18}O_z$+ $C_{10}H_{17}NO_z$) as a function of the calculated RO_2·+HO_2· contribution to the RO_2· bimolecular reaction rate. Linear fit is forced through the 1-to-1 point as in a hypothetical system with the RO_2·+HO_2· termination contributing 100 %, $C_{10}H_{18}O_z$ is the only unambiguous $C_{10}H_{17}O_x$· product and therefore would contribute 100 % to the $C_{10}H_{17}O_x$· product sum.

Within the above-described limits, the expected linear trend between $C_{10}H_{18}O_z$ contribution and the importance of RO_2·+HO_2· termination reactions can be observed. The good correlation between the expected contribution to HOM-RO_2· termination pathways in the framework and the actual observed HOM product distribution for both products from NO and HO_2· show that at least for relative considerations our simple generic chemical framework is able to capture the actual termination to closed shell products.

4.2. Interruption of the autoxidation chain

The second important framework parameter is the overall bimolecular reaction rate. Fast bimolecular reaction can result in an earlier end of the autoxidation process if it leads to closed shell products. In this case, less HOM compounds will be produced, and a reduction of the overall HOM signal will be observed. The change of overall HOM signal in the different chemical regimes in comparison to the RO_2· dominated base case with low bimolecular reaction rate is shown in **Fig. 5a)** as a function of the total bimolecular reaction rate. All compared conditions were normalized by the α-pinene ·OH turnover to ensure direct comparability.

https://doi.org/10.5194/egusphere-2026-4788
Preprint. Discussion started: 13 August 2026

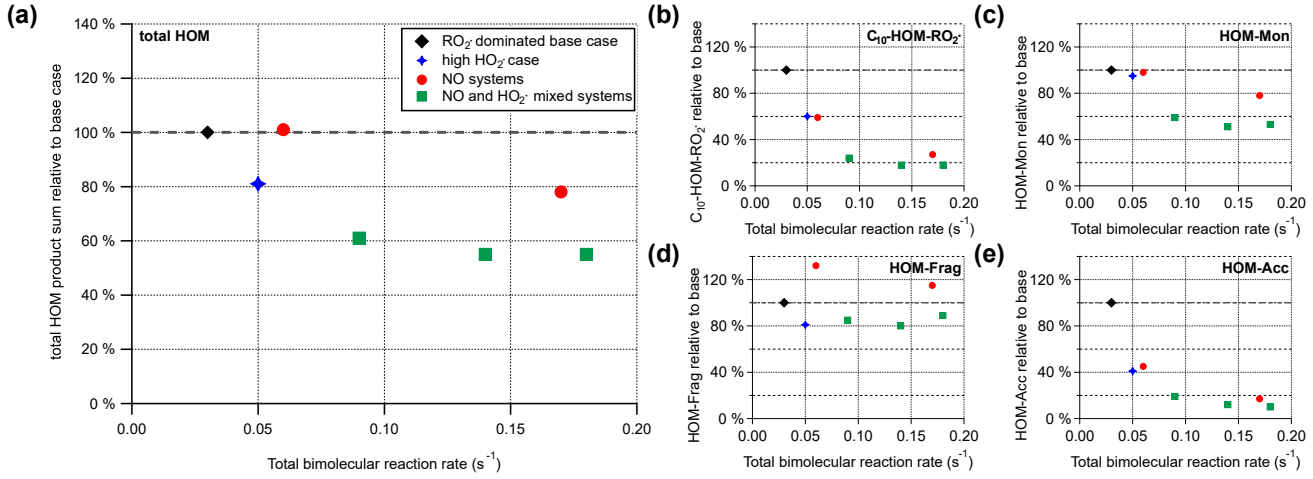

Figure 5 Relative change in HOM signal for the different chemical regimes compared to the base case in unseeded systems (all data normalized to α-pinene ·OH turnover) as a function of the total bimolecular reaction rate. Marker shape and color indicate chemical system. a) sum of all HOM products b) sum of C_{10}-HOM-RO_2·, has to be used cautiously as the detection of HOM-RO_2· is impacted by the presence of ON-HOM (for details see Supplement S4). c) sum of HOM-Mon d) sum of HOM-Frag e) sum of HOM-Acc.

Figure 5a) shows that the HOM suppression effect is significant but limited: While the bimolecular reaction rate increased by a factor of about six, the maximum reduction observed in the overall HOM sum was less than a factor of two compared to the base case. Furthermore, the decrease in HOM seems to level off at higher pseudo-first order bimolecular reaction rates.

A look at the different chemical systems shows the different effects of NO and HO_2·. The systems with high HO_2· (both, only HO_2· and HO_2· + NO) seem to fall along one curve, while the pure NO systems at comparable termination sink rates show less suppression of HOM. The smaller effect of NO at similar bimolecular reaction rates shows that reaction with NO does not exclusively lead to termination of the autoxidation chain, while the reaction with HO_2· often does. This is expected due to the formation and isomerization of alkoxy radicals which, as recently shown by Kang et al. (2025), can be important to the continuation of the autoxidation chain due to the occurrence of alkoxy-peroxy steps (see **Fig. 1**). This continuation of the autoxidation chain through alkoxy radicals could also explain the off-leveling in HOM reduction observed with increasing bimolecular reaction rate due to NO, though of course competitive autoxidation rates higher than 0.17 s^{-1} will also play a role. Additionally, as discussed in Baker et al. (2024), the presence of HO_2· leads to a stronger than expected reduction in HOM due to missing $C_{10}H_{15}O_x$-HOM-RO_2· formation. $C_{10}H_{15}O_x$-RO_2· have been observed as a major pathway for HOM formation in the α-pinene oxidation system (Kang et al., 2025; Shen et al., 2022). The specific pathways leading to $C_{10}H_{15}O_x$-HOM-RO_2· formation are expected to be dependent on alkoxy radical steps along the reaction pathway, both when starting from first-generation α-pinene oxidation products like pinonaldehyde (MCM mechanism, (Jenkin et al., 1997; Saunders et al., 2003)), and when assuming an H-abstraction from α-pinene (Shen et al., 2022; Wang et al., 2026). Thus, in systems dominated by HO_2· the reduced HOM formation can be explained by the decrease in alkoxy radical formation and the therefore missing $C_{10}H_{15}O_x$· pathway. The shift between $C_{10}H_{15}O_x$· and $C_{10}H_{17}O_x$· is further discussed in **Sec. 4.4**.

https://doi.org/10.5194/egusphere-2026-4788
Preprint. Discussion started: 13 August 2026

In conclusion, both, the pure NO and $HO_2\cdot$ cases illustrate the importance of crucial bimolecular reaction steps along the HOM formation pathways, and how such steps have to be considered to understand the SOA formation potential of a given system. Furthermore, they highlight the important role of alkoxy radicals in the autoxidation chain. The role of alkoxy radicals becomes even clearer when looking at the changes in specific product classes in the different systems, which are discussed in the next section.

4.3. Shift in the HOM-product distribution

Figure 5b) to **5e)** show the behavior of the individual product classes with increasing bimolecular reaction rate for the different chemical regimes. The C_{10}-HOM-$RO_2\cdot$ sum (**Fig. 5b**)) and the HOM-Acc sum (**Fig. 5c**)) decrease consistently and reach a stable level, showing no significant differences between the pure NO and the other systems. The decrease and their similar behavior are consistent with our expectations. Higher bimolecular reaction rates suppress the formation of HOM-$RO_2\cdot$ by autoxidation and present a sink for already formed HOM-$RO_2\cdot$. As HOM-Acc can only be formed by $RO_2\cdot$+$RO_2\cdot$ they follow the same trend. As mentioned in the previous section, it is interesting that the decrease seems to approach asymptotically a finite value, as this is likely caused by persistent autoxidation forming HOM-$RO_2\cdot$ with rates faster than 0.17 s^{-1} and the reformation of HOM-$RO_2\cdot$ via alkoxy-peroxy steps.

The HOM-Mon signal sum shows a behavior close to that observed for the total HOM sum in the systems containing NO, but no significant reduction in the high $HO_2\cdot$ case (for a detailed discussion of the $HO_2\cdot$ case see Baker et al. (2024)).

Especially interesting is the behavior of the HOM-Frag class, as here we see a different behavior compared to the other product classes: No clear decreasing trend can be observed, on the opposite, even at high bimolecular reaction rates an increase can still be seen in the high NO system. The major HOM-Frag formation pathway comprises alkoxy radicals which mainly stem from either $RO_2\cdot$+$RO_2\cdot$ or $RO_2\cdot$+NO. Supplement **Fig. S4** shows the change of the HOM-Frag sum compared to the base case as a function of the sum of the generic reaction rates for $RO_2\cdot$+$RO_2\cdot$ and $RO_2\cdot$+NO, with the color scale indicating the overall bimolecular reaction rate shown on the x-axis in **Fig. 5**. This visualization shows that for the fragment formation it is very important if pathways into alkoxy formation are available, with the overall bimolecular reaction rate playing only a secondary role. However, absolute comparisons are limited at much larger bimolecular reaction rates compared to the base case since changes due to missing HOM sources combine with changes due to different HOM-$RO_2\cdot$ termination pathways.

The importance of the HOM-Frag formation with NO in the system is also visible in the relative contribution of the product classes. While the contribution of HOM-Mon stayed approximately constant in all cases, a shift from HOM-Acc to HOM-Frag contribution was observed with increasing NO (see Supplement **Fig. S5**). In comparison, in the high $HO_2\cdot$ system a shift in the HOM product distribution from HOM-Acc to HOM-Mon was observed (Baker et al., 2024).

https://doi.org/10.5194/egusphere-2026-4788
Preprint. Discussion started: 13 August 2026

4.4. Contribution of $C_{10}H_{15}O_x\cdot$ and $C_{10}H_{17}O_x\cdot$ formation pathways to HOM

NO and $HO_2\cdot$ are expected to have opposite effects on the formation of alkoxy radicals. While NO facilitates the alkoxy formation, reactions of $HO_2\cdot$ with $RO_2\cdot$ have – with exceptions - minor or no pathway into alkoxy radicals and thus suppresses alkoxy formation compared to the base and NO cases. This should influence the HOM-$RO_2\cdot$ families available in the reaction system, as alkoxy radical steps are involved in $C_{10}H_{15}O_x\cdot$ formation (see **Sec. 4.2**). In contrast, $C_{10}H_{17}O_x\cdot$ is expected to be formed during autoxidation directly starting from α-pinene, and no alkoxy radical formation is necessary in the classical autoxidation chain. Thus, the main sources of closed-shell HOM products are expected to shift with the changes in the chemical regime leading to shifts in the product distribution. To specifically investigate the effect of NO on the system, we start the discussion with the results from the NO system (for results of the $HO_2\cdot$ system see Baker et al. (2024)), before moving on to account for the NO and $HO_2\cdot$ mixed cases.

Figure 6a) shows the contribution of the different HOM-Mon families to the non-ON HOM-Mon product sum in the NO system. As $C_{10}H_{18}O_z$ can only be formed from $C_{10}H_{17}O_x$-HOM-$RO_2\cdot$, and $C_{10}H_{14}O_z$ can only be formed from $C_{10}H_{15}O_x$-HOM-$RO_2\cdot$, the contributions of these families give the best indication of the importance of their radical precursor families. In contrast, $C_{10}H_{16}O_z$ products can be formed by both C_{10}-HOM-$RO_2\cdot$ precursor families. Therefore, in the case with NO if a precursor family has a specific fast pathway into $C_{10}H_{16}O_z$ that was not important in the base case, the HOM-Mon family contributions are no longer a good indicator. $C_{10}H_{16}O_z$ is also formed by internal termination (**Sec. 2.1** and Supplement **Fig. S1**), which we will discuss in the next section (**Sec. 4.5**).

The contribution of $C_{10}H_{16}O_z$ did not significantly change, while a clear decrease in contribution by $C_{10}H_{18}O_z$ and an increase in contribution by $C_{10}H_{14}O_z$ was observed with increasing NO. At high NO, the contribution of $C_{10}H_{18}O_z$ decreased to below 10 %, while $C_{10}H_{14}O_z$ contributed around 50 %. In comparison, in the NO_x-free base case $C_{10}H_{14}O_z$ contributed around 30 %.

https://doi.org/10.5194/egusphere-2026-4788
Preprint. Discussion started: 13 August 2026

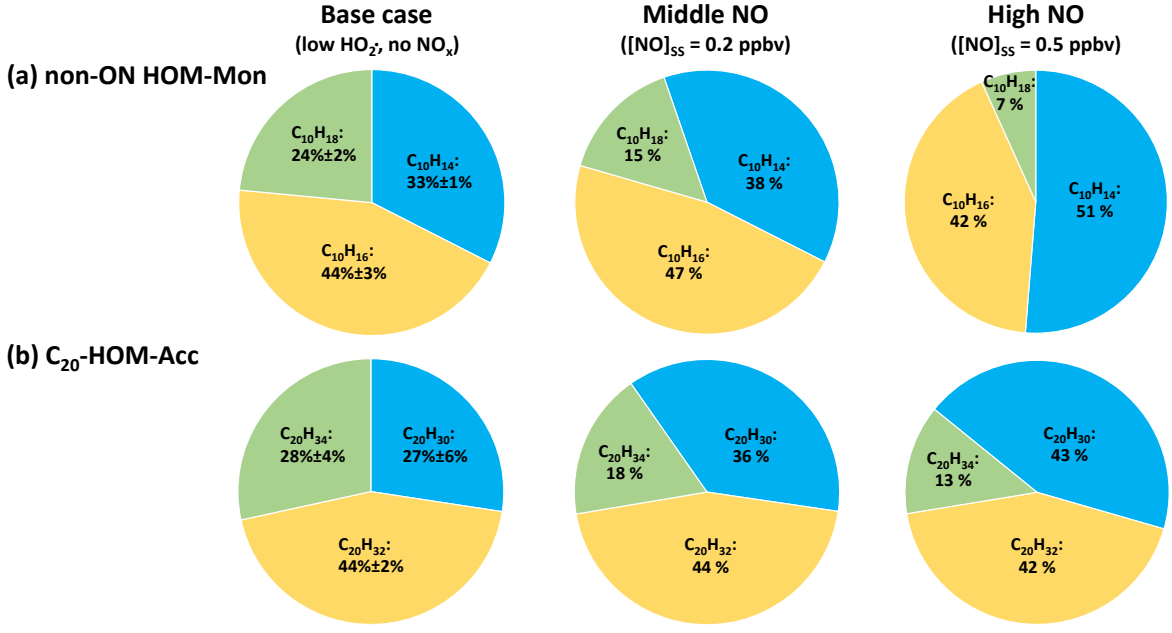

Figure 6 Contribution of a) the $C_{10}H_{14}O_z$, $C_{10}H_{16}O_z$ and $C_{10}H_{18}O_z$ families to the non-ON HOM-Mon and b) the $C_{20}H_{30}O_z$, $C_{20}H_{23}O_z$ and $C_{20}H_{34}O_z$ families to the C_{20}-HOM-Acc in the base case and at the two NO levels in the NO system (unseeded experiments).

This clear shift towards $C_{10}H_{14}O_z$ indicates a growing importance of the $C_{10}H_{15}O_x$-HOM-$RO_2\cdot$ in the non-ON products. This indication is corroborated by the observations in the C_{20}-HOM-Acc products shown in **Fig. 6b)**. Here, we see a similar trend: the contribution of $C_{20}H_{30}O_z$-HOM-Acc, which are formed from two $C_{10}H_{15}O_x$-$RO_2\cdot$, increased with NO availability, while the contribution of $C_{20}H_{34}O_z$-HOM-Acc, which are formed from two $C_{10}H_{17}O_x$-$RO_2\cdot$, decreased. The $C_{20}H_{32}O_z$-HOM-Acc, which are formed from both radical families, remained about the same.

As a hypothesis we propose that the increased importance of $C_{10}H_{15}O_x\cdot$ products compared to $C_{10}H_{17}O_x\cdot$ is due to the increased importance of alkoxy radical formation in systems with higher availability of NO. A further possibility could be a fast pathway of $C_{10}H_{17}O_x$-HOM-$RO_2\cdot$ into ON-HOM formation (fast compared to ON-HOM formation from $C_{10}H_{15}O_x\cdot$). Such a pathway would result in less contribution of $C_{10}H_{17}O_x\cdot$ products to non-ON species.

To exclude this possibility, we compare the ratio of ON-products formed by the two HOM-$RO_2\cdot$ families in relation to the contribution of $RO_2\cdot$+NO in both the pure NO and the mixed system (**Fig. 7**). The ON-HOMs investigated are $C_{10}H_{15}NO_z$ for $C_{10}H_{15}O_x\cdot$ and $C_{10}H_{17}NO_z$ for $C_{10}H_{17}O_x\cdot$. In **Fig. 7** two types of systems are separated: Systems, where the bimolecular $RO_2\cdot$ termination is strongly dominated by NO and $HO_2\cdot$ ($RO_2\cdot$+$RO_2\cdot$ < 5 %), and systems with a higher importance of $RO_2\cdot$+$RO_2\cdot$. This separation is helpful as alkoxy radical formation is also expected from $RO_2\cdot$+$RO_2\cdot$, which would also increase the importance of $C_{10}H_{15}O_x\cdot$.

https://doi.org/10.5194/egusphere-2026-4788
Preprint. Discussion started: 13 August 2026

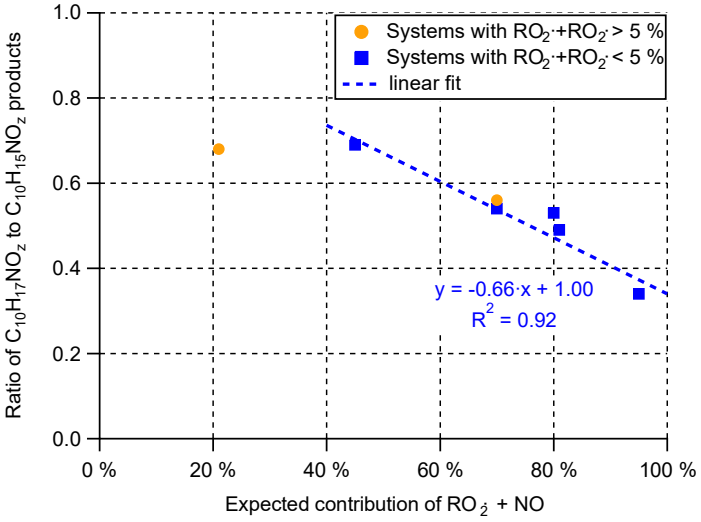

Figure 7 Ratio of the sum of all $C_{10}H_{17}NO_z$ products to the sum of all $C_{10}H_{15}NO_z$ products as a function of the expected RO_2·+NO contribution. Data set is separated by expected importance of RO_2·+RO_2· reactions (threshold 5 %). Linear fit applies to systems with RO_2·+RO_2· < 5 %.

With increasing contribution of RO_2·+NO the ratio of $C_{10}H_{17}NO_z$ to $C_{10}H_{15}NO_z$ decreases, indicating no fast pathway of $C_{10}H_{17}O_x$·+NO into ON formation, as then the opposite trend would be expected. Thus, the shift towards $C_{10}H_{15}O_x$· is observed in non-ON HOM-Mon, HOM-Acc, and ON-HOM, indicating that there is indeed a shift in the importance of the two radical precursor families. Similar comparisons can be found in the Supplement **Sec. S11** for the non-ON HOM-Mon and the C_{20}-HOM-Acc.

In conclusion, the available RO_2· reaction partners influence not only the HOM-RO_2· termination pathway, but also which HOM-RO_2· families are formed. In general, systems with a high significance of alkoxy radical formation, either by RO_2·+NO or RO_2·+RO_2·, show a lower importance of $C_{10}H_{17}O_x$·, i.e., the RO_2· radical family which is formed directly from an ·OH addition to α-pinene. Instead, the $C_{10}H_{15}O_x$· family is of higher importance. This observation may help bridge the gap between the high importance of $C_{10}H_{15}O_x$· HOM-products reported for α-pinene + ·OH experiments in atmospheric simulation chambers (Shen et al., 2022; Kang et al., 2025) and the dominance of $C_{10}H_{17}O_x$· reported from flow-tube studies focusing on the early reaction steps (Berndt et al., 2016; Berndt, 2021).

4.5. Indications for the importance of internal termination for RO_2· and RO·

Internal termination of HOM-RO_2· is another potentially significant termination pathway. To investigate the importance of this pathway, we can compare the observed decrease of closed shell products to the expected decrease.

This approach is based on the principle that in steady state the concentration of a bimolecular reaction product is defined by $[Product]_{SS}=k\cdot[Reactant(A)]_{SS}\cdot[Reactant(B)]_{SS}$, i.e., by the product of the precursor concentrations. For the formation of carbonyl products from RO_2·+RO_2· like $C_{10}H_{14}O_z$ from $C_{10}H_{15}O_x$·, this means that the relative decrease in the steady-state

https://doi.org/10.5194/egusphere-2026-4788
Preprint. Discussion started: 13 August 2026

concentration must reflect the decrease observed in their precursor HOM-RO_2·. Further decrease is expected if the steady-state concentrations of both reaction partners are decreased, as is the case for RO_2·+RO_2· reactions in our comparison between the RO_2·+RO_2· dominated base case and systems with higher importance of NO and HO_2·.

In the system with high HO_2· the decrease of $C_{10}H_{14}O_z$ was similar to the decrease measured in $C_{10}H_{15}O_x$·, but smaller than the decrease expected for the formation via RO_2·+RO_2·, since there was a reduction in both reaction partners ($C_{10}H_{15}O_x$-HOM-RO_2· and the RO_2· pool). This led to the hypothesis that internal termination of $C_{10}H_{15}O_x$-HOM-RO_2· may be an important formation pathway for $C_{10}H_{14}O_z$-HOM (Baker et al., 2024).

In the system with NO the observed decrease of $C_{10}H_{14}O_z$ was even significantly smaller than the decrease observed in $C_{10}H_{15}O_x$-HOM-RO_2·. An overview of the changes in all HOM-Mon families between NO cases and the base case can be found in Supplement **Fig. S9**. The $C_{10}H_{15}O_x$-HOM-RO_2· decreased by around 50 % and 70 % of the RO_2·+RO_2· dominated system in the middle and high NO case. Furthermore, from our model calculations a strong reduction in the overall available RO_2· is expected with the RO_2· pool decreasing by around 70 % (middle NO) and 90 % (high NO) of the RO_2·+RO_2· dominated system (for modeled RO_2· concentrations see Supplement **Tab. S5**). And yet the $C_{10}H_{14}O_z$ family signal only decreased by 20 % (middle NO) and 50 % (high NO) compared to the RO_2·+RO_2· dominated system. This persistence of $C_{10}H_{14}O_z$ cannot be explained even when assuming an internal termination pathway for $C_{10}H_{15}O_x$-HOM-RO_2·, as then the $C_{10}H_{14}O_z$ family signal should still be reduced at least by as much as the $C_{10}H_{15}O_x$-HOM-RO_2· family signal.

A possible explanation for this smaller-than-expected reduction in $C_{10}H_{14}O_z$ compared to $C_{10}H_{15}O_x$· is an internal termination pathway for alkoxy radicals. In this case $C_{10}H_{14}O_z$ would be formed from a $C_{10}H_{15}O_{x-1}$· alkoxy radical. This could explain our observations, as alkoxy radicals represent a sink for the observed $C_{10}H_{15}O_x$-HOM-RO_2· but are too reactive to be directly measured. The $C_{10}H_{15}O_{x-1}$· alkoxy radical could undergo internal termination analogous to the mechanism proposed by Rissanen et al. (2014) for RO_2· shown in Supplement **Fig. S1**. In this case, an intramolecular H-shift would lead to the formation of an alcohol group from the alkoxy radical. The resulting alkyl radical attached to the hydroperoxide group would form a carbonyl, and ·OH would be lost from the molecule. Another potential source of $C_{10}H_{14}O_z$ discussed for the particle phase is the hydrolysis and loss of HNO_3 from $C_{10}H_{15}NO_z$, (Takeuchi and Ng, 2019), however, such reactions may not be likely in the gas phase. Further investigations are necessary to fully elucidate the reason for the unexpected behavior of the $C_{10}H_{14}O_z$ family. However, formation through internal termination of alkoxy radicals offers an intriguing explanation.

4.6. Impact on product volatility and SOA formation potential

The previous sections discussed in detail how NO and HO_2· availability influences HOM formation pathways. We now address the question of how these changes in the HOM product distribution influence the formation of SOA. In general, there are two major factors which will lead to a reduction in observed SOA formation: Firstly, if less HOM products are produced, naturally less SOA will be produced as well. Secondly, if the formed HOM products have a higher volatility, they are more likely to stay in the gas phase, and the SOA amount produced will be reduced as well. Note, if a compound with a given volatility

https://doi.org/10.5194/egusphere-2026-4788
Preprint. Discussion started: 13 August 2026

partitions into the particle phase depends on the available organic mass concentration (Donahue et al., 2006; Stolzenburg et al., 2022).

In Baker et al. (2024) we already showed for the high $HO_2\cdot$ system that there is no significant change in the volatility of the produced HOMs, and that the main source of SOA suppression is the missing HOM-Acc formation compared to the base case. The same experimental strategy is now applied to test for a volatility shift in the systems with NO. In short, the gas-phase HOM product distribution is measured in steady state under two conditions: Once in the absence of ammonium sulfate seed particles, and once in the presence of ammonium sulfate seed particles. The HOM compounds with low enough volatility condense on the available particle surface, and we compare their fraction remaining in the gas phase as a proxy of their volatility. Consequently, the fraction remaining of either specific molecular formulas or product sums can be compared between reaction systems. In the system with NO, the ON-HOM present a new product class, providing a broader product distribution compared to the $RO_2\cdot$ dominated base case and the system with high $HO_2\cdot$.

Figure 8a) shows the fraction remaining in the gas phase as a function of the molar mass of each detected HOM. The data shown is from the mixed system with $HO_2\cdot$ and NO, with higher contribution to the bimolecular reactions by NO. This experiment was chosen to get a good representation of the ON-HOM. Information about particle size distributions and particle-phase concentrations for all investigated systems can be found in Supplement **Sec. S13**.

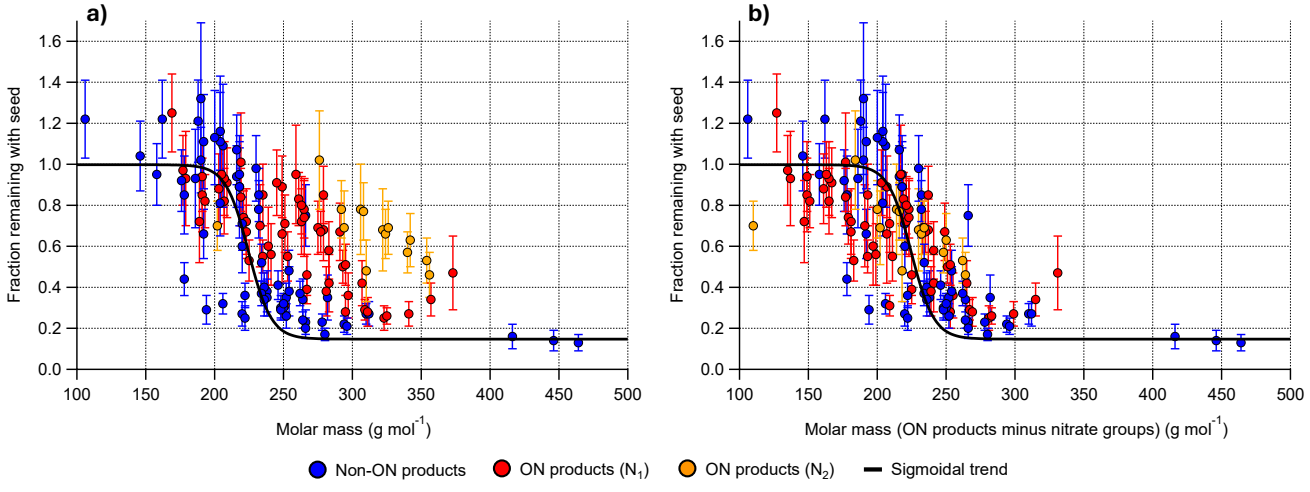

Figure 8 Gas-phase fraction remaining in presence of seed for the high NO, high $HO_2\cdot$ case (bimolecular reaction rate 0.18 s^{-1}, contribution by NO 81 %, by $HO_2\cdot$ 18 %). a) all HOM-compounds, b) all HOM-compounds with organic nitrate's molar mass being shifted by the nitrate termination group (NO_2) to ($M-46\ g\ mol-1$) for compounds containing one nitrate group (red markers) and to ($M-92\ g\ mol-1$) for compounds with two nitrate groups (orange markers). All data normalized with α-pinene $\cdot OH$ turnover. Markers represent compounds that were detected with relative standard deviation <30 %. Error bars represent results of error propagation (see Supplement Sec. S13)

The decrease of the fraction remaining with increasing molar mass of products shows clear differences between product classes. ON-HOMs show higher fractions remaining at the same molar masses compared to HOMs containing no nitrogen. Indeed, it seems that the nitrate termination group does not result in the same decrease of volatility as the non-ON termination

https://doi.org/10.5194/egusphere-2026-4788
Preprint. Discussion started: 13 August 2026

groups (hydroperoxide, carbonyl or alcohol). As a result, the volatility of an ON-HOM is more comparable to a non-ON HOM of lower molar mass. Interestingly, **Fig. 8b)** shows that a more similar trend between non-ON and ON compounds is achieved if the weight of the nitrate termination group is subtracted from the ON-HOM's molar mass to compare it to a carbonyl HOM formed from the same precursor. This observation fits the results published by Pullinen et al. (2020), who concluded that a non-ON and an ON product from the same HOM-RO_2· precursor shows no significant difference in effective uptake coefficients, even though the ON product has a higher oxygen number and is heavier. The smaller than expected decrease in volatility compared to non-ON termination products could potentially be connected to missing hydrogen bonds from the organic nitrate group. Sagawa and Shikata (2014) showed that nitro groups do not form strong hydrogen bonds with water molecules. While we focused on volatility in our analysis, another important parameter impacting the gas-to-particle partitioning could thus be the solubility. Suda et al. (2014) showed that nitrate functionalization led to a decrease in hygroscopicity. All experiments in this work were performed at the same humidity level, however experiments at different humidity levels would help to elucidate the effect of solubility.

Further hints towards higher volatility of ON-HOM can be found in Presto et al. (2005), who found higher volatility of ON studying α-pinene ozonolysis, and in Graham et al. (2023), who reported higher volatility of α-pinene+NO_3 derived SOA compared to α-pinene+O_3 derived SOA.

In comparison to the fraction remaining plot for the RO_2· dominated base, and the high HO_2· case (Baker et al., 2024), we can see even further suppression of HOM-Acc, as only three compounds remain in the high molar mass range which fulfill the plotting criteria of a significant signal increase compared to the background upon oxidation start and an average steady-state signal with a relative standard deviation <30 %. We also observe a further shift towards lighter HOM-Frag compounds, which additionally often show higher fractions remaining than the HOM-Frag observed in the base case. In conclusion, a higher volatility of the HOM product distribution in the system with NO compared to the base case is expected mainly due to three reasons: Suppression of low volatility HOM-Acc products, a shift towards higher volatility HOM-Frag products, and the formation of ON-HOM, which have higher volatility than the respective non-ON closed shell products.

To assess the overall effect of these factors on SOA formation we calculated the wall-loss-corrected SOA yields for all cases as described by Sarrafzadeh et al. (2016) (for details on the calculation see Supplement **Sec. S15,** for the utilized data see **Sec. S13).** The result as a function of the generic total bimolecular reaction rate of each case is shown in **Fig. 9**. The SOA yield is dependent on many factors including temperature, available organic aerosol mass concentration, and of course VOC+·OH turnover. However, the experiments here were performed to be comparable (constant temperature, approximately same turnover, low organic aerosol mass concentrations in all cases) allowing a direct relative comparison. **Figure 9** shows that with increasing bimolecular reaction rate the SOA yield decreases before reaching a stable level. Significant reductions in SOA yield were observed with maximum reductions of circa a factor of two. This may also be an estimator for the bias of SOA yields if results from RO_2· dominated laboratory systems are directly transferred to atmospheric situations, where HO_2· and NO dominate. However, as discussed in **Sec. 4.2**, in comparison the bimolecular reaction rate increased by circa a factor of

https://doi.org/10.5194/egusphere-2026-4788
Preprint. Discussion started: 13 August 2026

six, showing the persistence of SOA formation. Interestingly, while marker shape and color in **Fig. 9** indicate the chemical system, all systems seem to fall along one trend line.

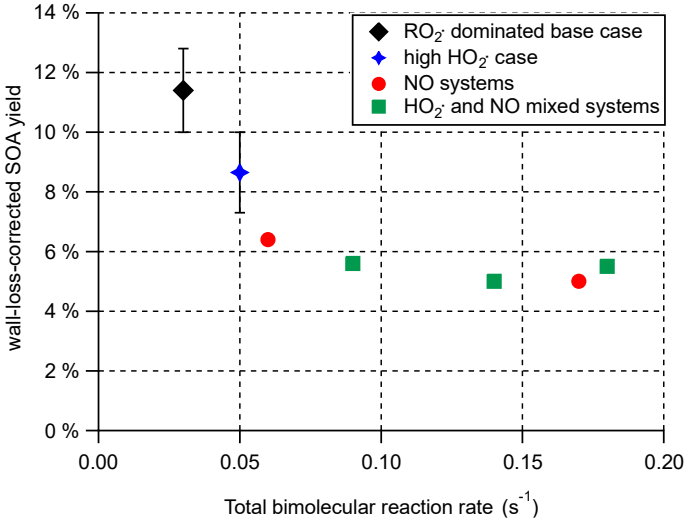

Figure 9 Wall-loss corrected SOA yield in the different chemical regimes as a function of the total bimolecular reaction rate. Error bars indicate observed variation of repetitions.

This is different compared to the overall gas-phase HOM product sum (**Fig. 5a)**), where the pure NO system showed smaller reductions than systems with higher $HO_2\cdot$ availability. The development of the SOA yield with increasing bimolecular reaction rate instead resembles the decrease shown for the C_{10}-HOM-$RO_2\cdot$ and the HOM-Acc product signal in the gas phase (see **Fig. 5b)** and **5e)**). This difference is explained by our previous considerations regarding product volatility. In the system with NO, the overall amount of gas-phase HOM products produced was not or not as strongly reduced, however, the produced products had lower molar masses and higher volatilities (HOM-Frag and ON-HOM) in comparison to the $RO_2\cdot$ dominated base case leading to a smaller SOA formation potential.

5. Conclusion

This study utilized generic $RO_2\cdot$ and recent HOM formation chemistry to develop experiments and data analysis approaches, with the goal to bridge the gap between the understanding of mechanistic pathways determined in laboratory experiments and SOA formation in the real atmosphere. We investigated changes in HOM and SOA formation across a range of reaction conditions. To this end, the bimolecular $RO_2\cdot$ reaction rate as well as the contribution of $HO_2\cdot$, NO, and $RO_2\cdot$ to it were varied. At the same time, the α-pinene OH turnover was kept constant to keep the entry channel into HOM formation constant as well. By detailed analysis of the HOM product distribution under different experimental conditions, we determined important factors influencing the SOA formation potential. Two such factors are the molar mass and volatility of the formed oxidation products. While HOM accretion product formation increases the SOA formation potential, formation of HOM fragments and organic

https://doi.org/10.5194/egusphere-2026-4788
Preprint. Discussion started: 13 August 2026

nitrate containing HOM products can decrease it. Targeted seeding experiments revealed that organic nitrate HOM products partition less into the particle phase compared to non-nitrogen containing HOM products of similar molar mass. Both, the extend of formation and the partitioning behavior of organic nitrate HOM observed in this study, agree well with results previously published by Pullinen et al. (2020).

The study presented here highlights the important role of alkoxy radical formation. Alkoxy radicals are mainly formed from RO_2·+NO or RO_2·+RO_2· and influence the HOM product distribution in multiple ways. On one hand, alkoxy radicals can fragment, forming HOM-Frag and decreasing the SOA formation potential. On the other hand, alkoxy radicals can undergo alkoxy-peroxy steps, which, as our results show, are an integral part of autoxidation under atmospheric conditions. Our results regarding the importance of alkoxy radical chemistry are in line with recent works (Wang et al., 2021; Kang et al., 2025). Alkoxy-peroxy steps are responsible for HOM formation pathways from $C_{10}H_{15}O_x$· and facilitate continuation of the autoxidation chain, even at high bimolecular reaction rates. In contrast, in systems which have high bimolecular reaction rates due to the reaction of RO_2·+HO_2·, such alkoxy radical pathways are missing.

Reaction regimes with low bimolecular RO_2 reaction rates and high importance of RO_2+RO_2 reactions showed the highest HOM production and SOA yields. However, moving away from RO_2+RO_2 dominated reaction systems towards higher bimolecular reaction rates and increasing importance of RO_2+NO led to a maximum decrease in HOM production of only 45 %. At the same time, the maximum decrease in SOA yield was about 50 %. This persistent HOM formation could be caused by both, fast RO_2· intramolecular H-shifts during autoxidation, and the importance of alkoxy-peroxy steps. Here additional experiments with large bimolecular reaction rates due to RO_2·+HO_2· could help to elucidate the role of fast intramolecular H-shifts.

Even for increases in the RO_2· bimolecular reaction rate by up to a factor of six the decrease in SOA yield stabilized at a maximum factor of circa two, which could be an estimator for the bias of SOA yields from RO_2· dominated laboratory systems compared to more realistic conditions, which are in general dominated by HO_2· and NO.

The methodological approach of characterizing the reaction regime in combination with mechanistic considerations of known HOM-RO_2· chemistry provide a conclusive picture of the HOM-RO_2· reaction pathways. Our work presents a compelling argument for utilizing the expected overall bimolecular RO_2· reaction rate, as well as the contributions by HO_2·, NO, and RO_2· reactions, not only for experimental design, but also for the interpretation and transfer of experimental results to the real atmosphere in models. This work focuses on the α-pinene+OH system as an example, but similar effects can be expected for all monoterpenes. It will thus be useful to extend the characterization framework. This will of course require a well characterized generic chemistry of the precursor VOC, which, however, may become possible with advances in automated mechanism generation (Vereecken et al., 2018; Aumont et al., 2005; Aumont et al., 2026). A next step could then also be the extension to more complex systems with strong sources of small RO_2· radicals, like CH_3O_2·.

Our findings highlight that bimolecular reactions do not only represent an interruption in HOM formation, but also open new formation pathways by reaction of (HOM-)RO_2·+NO, leading to fast alkoxy and then peroxy radical formation. This has interesting and important implications for HOM formation in the atmosphere: While in general termination is the main

https://doi.org/10.5194/egusphere-2026-4788
Preprint. Discussion started: 13 August 2026

expected reaction outcome of RO_2·+NO for lower-oxidized "conventional" RO_2·, the same is not necessarily the case for HOM-RO_2·. Indeed, more "urban" atmospheric conditions with higher availability of NO might be more efficient in SOA formation than previously assumed, while the current understanding of more "pristine" environments with high importance of HO_2· could lack critical pathways into HOM formation.

Data availability

The data to reproduce the figures can be found in https://doi.org/10.26165/JUELICH-DATA/7ZLI6P (Baker et al., 2026). Data providing information on the particle-phase concentrations and model results for each steady state, as well as peak lists showing the (HOM) analytes identified in the NO_3-CIMS mass spectra can be found in the Supplement.

Author contribution

TFM, MH, SRZ, and GM conceptualized the study, and TFM, YB, SK, and SRZ designed the experiments. TFM and YB developed the analysis methodology. The experiments were performed by YB, VG, SK, and SRZ. Instrument deployment and/or data analysis were performed by YB, VG, HW, RW, AZ, QH, and SK. YB did model calculations of the experiments. AV, SPO, TJB, GM, and MH provided counsel on experiment design and data interpretation. The compiled data set was interpreted by YB and TFM, and the results were discussed by all co-authors. YB visualized the data, and YB and TFM prepared the manuscript. All co-authors reviewed the manuscript.

Competing interests

The authors declare no competing financial interest. One of the authors is a member of the editorial board of ACP.

Financial support

This research has received funding from the European Union's Horizon 2020 research and innovation program under the FORCeS project under grant agreement no. 821205, the German Federal Ministry of Education and Research (BMBF) under the FONA Strategy "Research for Sustainability" as part of the implementation of ACTRIS-D under the funding code 01LK200010, Vetenskapsrådet (VR, grant agreement no. 2018-04430), Svenska Forskningsrådet Formas (grant agreement no. 2019-586) and the UK Natural Environment Research Council (NERC) under grant agreement no. NE/V012665/1.

https://doi.org/10.5194/egusphere-2026-4788
Preprint. Discussion started: 13 August 2026

References

Albrecht, S. R., Novelli, A., Hofzumahaus, A., Kang, S., Baker, Y., Mentel, T., Wahner, A., and Fuchs, H.: Measurements of hydroperoxy radicals (HO2) at atmospheric concentrations using bromide chemical ionisation mass spectrometry, Atmos. Meas. Tech., 12, 891-902, https://doi.org/10.5194/amt-12-891-2019, 2019.

Atkinson, R. and Arey, J.: Atmospheric degradation of volatile organic compounds, Chem. Rev., 103, 4605-4638, https://doi.org/10.1021/cr0206420, 2003.

Aumont, B., Szopa, S., and Madronich, S.: Modelling the evolution of organic carbon during its gas-phase tropospheric oxidation: development of an explicit model based on a self generating approach, Atmos. Chem. Phys., 5, 2497-2517, 10.5194/acp-5-2497-2005, 2005.

Aumont, B., Valorso, R., Rickard, A., Jenkin, M., Lee-Taylor, J., Orlando, J., Madronich, S., Vereecken, L., and Camredon, M.: GECKO-A v1.0: Exploring VOC Oxidation Trajectories Through Comparison with the Master Chemical Mechanism, EGUsphere, 2026, 1-47, 10.5194/egusphere-2026-2907, 2026.

Baker, Y., Geretti, V., Kang, S., Wu, R., Wang, H., He, Q., Hohaus, T., Zanders, A., Bachner, M., Wu, C., Bannan, T. J., O'Meara, S. P., Voliotis, A., Hallquist, M., McFiggans, G., Zorn, S. R., and Mentel, T. F.: Supplementary data for the manuscript "Impact of the chemical regime on highly oxygenated molecule and secondary organic aerosol formation: Effects of varying the importance of NO, HO2·, RO2· reactions on α-pinene photooxidation products", Jülich DATA [dataset], https://doi.org/10.26165/JUELICH-DATA/7ZLI6P, 2026.

Baker, Y., Kang, S., Wang, H., Wu, R., Xu, J., Zanders, A., He, Q., Hohaus, T., Ziehm, T., Geretti, V., Bannan, T. J., O'Meara, S. P., Voliotis, A., Hallquist, M., McFiggans, G., Zorn, S. R., Wahner, A., and Mentel, T. F.: Impact of HO2/RO2 ratio on highly oxygenated α-pinene photooxidation products and secondary organic aerosol formation potential, Atmos. Chem. Phys., 24, 4789-4807, https://doi.org/10.5194/acp-24-4789-2024, 2024.

Berndt, T.: Peroxy Radical Processes and Product Formation in the OH Radical-Initiated Oxidation of α-Pinene for Near-Atmospheric Conditions, J. Phys. Chem. A, 125, 9151-9160, https://doi.org/10.1021/acs.jpca.1c05576, 2021.

Berndt, T., Richters, S., Jokinen, T., Hyttinen, N., Kurtén, T., Otkjaer, R. V., Kjaergaard, H. G., Stratmann, F., Herrmann, H., Sipila, M., Kulmala, M., and Ehn, M.: Hydroxyl radical-induced formation of highly oxidized organic compounds, Nat. Commun., 7, 13677, https://doi.org/10.1038/ncomms13677, 2016.

Bianchi, F., Garmash, O., He, X. C., Yan, C., Iyer, S., Rosendahl, I., Xu, Z. N., Rissanen, M. P., Riva, M., Taipale, R., Sarnela, N., Petäjä, T., Worsnop, D. R., Kulmala, M., Ehn, M., and Junninen, H.: The role of highly oxygenated molecules (HOMs) in determining the composition of ambient ions in the boreal forest, Atmos. Chem. Phys., 17, 13819-13831, https://doi.org/10.5194/acp-17-13819-2017, 2017.

Cho, C., Fuchs, H., Hofzumahaus, A., Holland, F., Bloss, W. J., Bohn, B., Dorn, H. P., Glowania, M., Hohaus, T., Liu, L., Monks, P. S., Niether, D., Rohrer, F., Sommariva, R., Tan, Z., Tillmann, R., Kiendler-Scharr, A., Wahner, A., and Novelli, A.: Experimental chemical budgets of OH, HO2, and RO2 radicals in rural air in western Germany during the JULIAC campaign 2019, Atmos. Chem. Phys., 23, 2003-2033, https://doi.org/10.5194/acp-23-2003-2023, 2023.

Crounse, J. D., Nielsen, L. B., Jørgensen, S., Kjaergaard, H. G., and Wennberg, P. O.: Autoxidation of organic compounds in the atmosphere, J. Phys. Chem. Lett., 4, 3513-3520, https://doi.org/10.1021/jz4019207, 2013.

Donahue, N. M., Robinson, A., Stanier, C., and Pandis, S.: Coupled partitioning, dilution, and chemical aging of semivolatile organics, Environ. Sci. Technol., 40, 2635-2643, https://doi.org/10.1021/es052297c, 2006.

Eddingsaas, N., Loza, C., Yee, L., Seinfeld, J., and Wennberg, P.: α-Pinene photooxidation under controlled chemical conditions – Part 1: Gas-phase composition in low- and high-NOx environments, Atmos. Chem. Phys., 12, 6489-6504, https://doi.org/10.5194/acp-12-6489-2012, 2012.

Ehn, M., Thornton, J. A., Kleist, E., Sipila, M., Junninen, H., Pullinen, I., Springer, M., Rubach, F., Tillmann, R., Lee, B., Lopez-Hilfiker, F., Andres, S., Acir, I. H., Rissanen, M., Jokinen, T., Schobesberger, S., Kangasluoma, J., Kontkanen, J., Nieminen, T., Kurtén, T., Nielsen, L. B., Jorgensen, S., Kjaergaard, H. G., Canagaratna, M., Maso, M. D., Berndt, T., Petaja, T., Wahner, A., Kerminen, V. M., Kulmala, M., Worsnop, D. R., Wildt, J., and Mentel, T. F.: A large source of low-volatility secondary organic aerosol, Nature, 506, 476-479, https://doi.org/10.1038/nature13032, 2014.

Franzon, L., Camredon, M., Valorso, R., Aumont, B., and Kurtén, T.: Ether and ester formation from peroxy radical recombination: a qualitative reaction channel analysis, Atmospheric Chemistry and Physics, 24, 11679-11699, https://doi.org/10.5194/acp-24-11679-2024, 2024.

https://doi.org/10.5194/egusphere-2026-4788
Preprint. Discussion started: 13 August 2026

Graham, E. L., Wu, C., Bell, D. M., Bertrand, A., Haslett, S. L., Baltensperger, U., El Haddad, I., Krejci, R., Riipinen, I., and Mohr, C.: Volatility of aerosol particles from NO3 oxidation of various biogenic organic precursors, Atmos. Chem. Phys., 23, 7347-7362, https://doi.org/10.5194/acp-23-7347-2023, 2023.

Hasson, A. S., Kuwata, K. T., Arroyo, M. C., and Petersen, E. B.: Theoretical studies of the reaction of hydroperoxy radicals (HO2) with ethyl peroxy (CH3CH2O2), acetyl peroxy (CH3C(O)O2), and acetonyl peroxy (CH3C(O)CH2O2) radicals, J. Photochem. Photobiol. A, 176, 218-230, https://doi.org/10.1016/j.jphotochem.2005.08.012, 2005.

Iyer, S., Reiman, H., Møller, K. H., Rissanen, M. P., Kjaergaard, H. G., and Kurtén, T.: Computational investigation of RO2+ HO2 and RO2+ RO2 reactions of monoterpene derived first-generation peroxy radicals leading to radical recycling, J. Phys. Chem. A, 122, 9542-9552, https://doi.org/10.1021/acs.jpca.8b09241, 2018.

Jenkin, M. E., Saunders, S. M., and Pilling, M. J.: The tropospheric degradation of volatile organic compounds: a protocol for mechanism development, Atmos. Environ., 31, 81-104, https://doi.org/10.1016/S1352-2310(96)00105-7, 1997.

Jenkin, M. E., Valorso, R., Aumont, B., and Rickard, A. R.: Estimation of rate coefficients and branching ratios for reactions of organic peroxy radicals for use in automated mechanism construction, Atmos. Chem. Phys., 19, 7691-7717, https://doi.org/10.5194/acp-19-7691-2019, 2019.

Kang, S., Wildt, J., Pullinen, I., Vereecken, L., Wu, C., Wahner, A., Zorn, S. R., and Mentel, T. F.: Formation of highly oxygenated organic molecules from α-pinene photooxidation: evidence for the importance of highly oxygenated alkoxy radicals, Atmospheric Chemistry and Physics, 25, 15715-15740, https://doi.org/10.5194/acp-25-15715-2025, 2025.

Kenagy, H. S., Heald, C. L., Tahsini, N., Goss, M. B., and Kroll, J. H.: Can we achieve atmospheric chemical environments in the laboratory? An integrated model-measurement approach to chamber SOA studies, Science Advances, 10, eado1482, https://doi.org/10.1126/sciadv.ado1482, 2024.

Kiendler-Scharr, A., Wildt, J., Maso, M. D., Hohaus, T., Kleist, E., Mentel, T. F., Tillmann, R., Uerlings, R., Schurr, U., and Wahner, A.: New particle formation in forests inhibited by isoprene emissions, Nature, 461, 381-384, https://doi.org/10.1038/nature08292, 2009.

McFiggans, G., Mentel, T. F., Wildt, J., Pullinen, I., Kang, S., Kleist, E., Schmitt, S., Springer, M., Tillmann, R., Wu, C., Zhao, D., Hallquist, M., Faxon, C., Le Breton, M., Hallquist, A. M., Simpson, D., Bergstrom, R., Jenkin, M. E., Ehn, M., Thornton, J. A., Alfarra, M. R., Bannan, T. J., Percival, C. J., Priestley, M., Topping, D., and Kiendler-Scharr, A.: Secondary organic aerosol reduced by mixture of atmospheric vapours, Nature, 565, 587-593, https://doi.org/10.1038/s41586-018-0871-y, 2019.

Mentel, T., Springer, M., Ehn, M., Kleist, E., Pullinen, I., Kurtén, T., Rissanen, M., Wahner, A., and Wildt, J.: Formation of highly oxidized multifunctional compounds: autoxidation of peroxy radicals formed in the ozonolysis of alkenes–deduced from structure–product relationships, Atmos. Chem. Phys., 15, 6745-6765, https://doi.org/10.5194/acp-15-6745-2015, 2015.

Nie, W., Yan, C., Yang, L., Roldin, P., Liu, Y., Vogel, A. L., Molteni, U., Stolzenburg, D., Finkenzeller, H., Amorim, A., Bianchi, F., Curtius, J., Dada, L., Draper, D. C., Duplissy, J., Hansel, A., He, X.-C., Hofbauer, V., Jokinen, T., Kim, C., Lehtipalo, K., Nichman, L., Mauldin, R. L., Makhmutov, V., Mentler, B., Mizelli-Ojdanic, A., Petäjä, T., Quéléver, L. L. J., Schallhart, S., Simon, M., Tauber, C., Tomé, A., Volkamer, R., Wagner, A. C., Wagner, R., Wang, M., Ye, P., Li, H., Huang, W., Qi, X., Lou, S., Liu, T., Chi, X., Dommen, J., Baltensperger, U., El Haddad, I., Kirkby, J., Worsnop, D., Kulmala, M., Donahue, N. M., Ehn, M., and Ding, A.: NO at low concentration can enhance the formation of highly oxygenated biogenic molecules in the atmosphere, Nat. Commun., 14, 3347, https://doi.org/10.1038/s41467-023-39066-4, 2023.

Noziere, B. and Barnes, I.: Evidence for formation of a PAN analogue of pinonic structure and investigation of its thermal stability, J. Geophys. Res. Atmos., 103, 25587-25597, https://doi.org/10.1029/98JD01677, 1998.

Otkjaer, R. V., Jakobsen, H. H., Tram, C. M., and Kjaergaard, H. G.: Calculated Hydrogen Shift Rate Constants in Substituted Alkyl Peroxy Radicals, J. Phys. Chem. A, 122, 8665-8673, https://doi.org/10.1021/acs.jpca.8b06223, 2018.

Peng, Z., Lee-Taylor, J., Orlando, J. J., Tyndall, G. S., and Jimenez, J. L.: Organic peroxy radical chemistry in oxidation flow reactors and environmental chambers and their atmospheric relevance, Atmos. Chem. Phys., 19, 813-834, https://doi.org/10.5194/acp-19-813-2019, 2019.

Peräkylä, O., Berndt, T., Franzon, L., Hasan, G., Meder, M., Valiev, R. R., Daub, C. D., Varelas, J. G., Geiger, F. M., Thomson, R. J., Rissanen, M., Kurtén, T., and Ehn, M.: Large gas-phase source of esters and other accretion products in the atmosphere, Journal of the American Chemical Society, 145, 7780-7790, https://doi.org/10.1021/jacs.2c10398, 2023.

Piletic, I. R. and Kleindienst, T. E.: Rates and yields of unimolecular reactions producing highly oxidized peroxy radicals in the OH-induced autoxidation of α-pinene, β-pinene, and limonene, J. Phys. Chem. A, 126, 88-100, https://doi.org/10.1021/acs.jpca.1c07961, 2022.

https://doi.org/10.5194/egusphere-2026-4788
Preprint. Discussion started: 13 August 2026

Presto, A. A., Huff Hartz, K. E., and Donahue, N. M.: Secondary Organic Aerosol Production from Terpene Ozonolysis. 2. Effect of NOx concentration, Environ. Sci. Technol., 39, 7046-7054, https://doi.org/10.1021/es050400s, 2005.
Pullinen, I., Schmitt, S., Kang, S., Sarrafzadeh, M., Schlag, P., Andres, S., Kleist, E., Mentel, T. F., Rohrer, F., Springer, M., Tillmann, R., Wildt, J., Wu, C., Zhao, D., Wahner, A., and Kiendler-Scharr, A.: Impact of NOx on secondary organic aerosol (SOA) formation from α-pinene and β-pinene photooxidation: the role of highly oxygenated organic nitrates, Atmos. Chem. Phys., 20, 10125-10147, https://doi.org/10.5194/acp-20-10125-2020, 2020.
Rissanen, M. P., Mikkilä, J., Iyer, S., and Hakala, J.: Multi-scheme chemical ionization inlet (MION) for fast switching of reagent ion chemistry in atmospheric pressure chemical ionization mass spectrometry (CIMS) applications, Atmos. Meas. Tech., 12, 6635-6646, https://doi.org/10.5194/amt-12-6635-2019, 2019.
Rissanen, M. P., Kurtén, T., Sipila, M., Thornton, J. A., Kangasluoma, J., Sarnela, N., Junninen, H., Jorgensen, S., Schallhart, S., Kajos, M. K., Taipale, R., Springer, M., Mentel, T. F., Ruuskanen, T., Petaja, T., Worsnop, D. R., Kjaergaard, H. G., and Ehn, M.: The formation of highly oxidized multifunctional products in the ozonolysis of cyclohexene, J. Am. Chem. Soc., 136, 15596-15606, https://doi.org/10.1021/ja507146s, 2014.
Roldin, P., Ehn, M., Kurtén, T., Olenius, T., Rissanen, M. P., Sarnela, N., Elm, J., Rantala, P., Hao, L., Hyttinen, N., Heikkinen, L., Worsnop, D. R., Pichelstorfer, L., Xavier, C., Clusius, P., Öström, E., Petäjä, T., Kulmala, M., Vehkamäki, H., Virtanen, A., Riipinen, I., and Boy, M.: The role of highly oxygenated organic molecules in the Boreal aerosol-cloud-climate system, Nat. Commun., 10, 4370, https://doi.org/10.1038/s41467-019-12338-8, 2019.
Sagawa, N. and Shikata, T.: Are all polar molecules hydrophilic? Hydration numbers of nitro compounds and nitriles in aqueous solution, Phys. Chem. Chem. Phys., 16, 13262-13270, https://doi.org/10.1039/C4CP01280A 2014.
Sanchez, J., Tanner, D. J., Chen, D., Huey, L. G., and Ng, N. L.: A new technique for the direct detection of HO2 radicals using bromide chemical ionization mass spectrometry (Br-CIMS): initial characterization, Atmos. Meas. Tech., 9, 3851-3861, https://doi.org/10.5194/amt-9-3851-2016, 2016.
Sarrafzadeh, M., Wildt, J., Pullinen, I., Springer, M., Kleist, E., Tillmann, R., Schmitt, S. H., Wu, C., Mentel, T. F., Zhao, D., Hastie, D. R., and Kiendler-Scharr, A.: Impact of NOx and OH on secondary organic aerosol formation from β-pinene photooxidation, Atmos. Chem. Phys., 16, 11237-11248, https://doi.org/10.5194/acp-16-11237-2016, 2016.
Saunders, S. M., Jenkin, M. E., Derwent, R., and Pilling, M.: Protocol for the development of the Master Chemical Mechanism, MCM v3 (Part A): tropospheric degradation of non-aromatic volatile organic compounds, Atmos. Chem. Phys., 3, 161-180, https://doi.org/10.5194/acp-3-161-2003, 2003.
Schervish, M. and Donahue, N. M.: Peroxy radical kinetics and new particle formation, Environ. Sci. Atmos., 1, 79-92, https://doi.org/10.1039/d0ea00017e, 2021.
Seinfeld, J. H. and Pandis, S. N.: Atmospheric Chemistry and Physics: from Air Pollution to Climate Change, 3, John Wiley & Sons, Hoboken, New Jersey, USA2016.
Shen, H., Vereecken, L., Kang, S., Pullinen, I., Fuchs, H., Zhao, D., and Mentel, T. F.: Unexpected significance of a minor reaction pathway in daytime formation of biogenic highly oxygenated organic compounds, Sci. Adv., 8, eabp8702, https://doi.org/10.1126/sciadv.abp8702, 2022.
Stolzenburg, D., Wang, M., Schervish, M., and Donahue, N. M.: Tutorial: Dynamic organic growth modeling with a volatility basis set, J. Aerosol Sci., 166, 106063, https://doi.org/10.1016/j.jaerosci.2022.106063, 2022.
Suda, S. R., Petters, M. D., Yeh, G. K., Strollo, C., Matsunaga, A., Faulhaber, A., Ziemann, P. J., Prenni, A. J., Carrico, C. M., Sullivan, R. C., and Kreidenweis, S. M.: Influence of functional groups on organic aerosol cloud condensation nucleus activity, Environ Sci Technol, 48, 10182-10190, https://doi.org/10.1021/es502147y, 2014.
Takeuchi, M. and Ng, N. L.: Chemical composition and hydrolysis of organic nitrate aerosol formed from hydroxyl and nitrate radical oxidation of α-pinene and β-pinene, Atmos. Chem. Phys., 19, 12749-12766, https://doi.org/10.5194/acp-19-12749-2019, 2019.
Tsigaridis, K., Daskalakis, N., Kanakidou, M., Adams, P. J., Artaxo, P., Bahadur, R., Balkanski, Y., Bauer, S. E., Bellouin, N., Benedetti, A., Bergman, T., Berntsen, T. K., Beukes, J. P., Bian, H., Carslaw, K. S., Chin, M., Curci, G., Diehl, T., Easter, R. C., Ghan, S. J., Gong, S. L., Hodzic, A., Hoyle, C. R., Iversen, T., Jathar, S., Jimenez, J. L., Kaiser, J. W., Kirkevåg, A., Koch, D., Kokkola, H., Lee, Y. H., Lin, G., Liu, X., Luo, G., Ma, X., Mann, G. W., Mihalopoulos, N., Morcrette, J. J., Müller, J. F., Myhre, G., Myriokefalitakis, S., Ng, N. L., O'Donnell, D., Penner, J. E., Pozzoli, L., Pringle, K. J., Russell, L. M., Schulz, M., Sciare, J., Seland, Ø., Shindell, D. T., Sillman, S., Skeie, R. B., Spracklen, D., Stavrakou, T., Steenrod, S. D., Takemura,

https://doi.org/10.5194/egusphere-2026-4788
Preprint. Discussion started: 13 August 2026

T., Tiitta, P., Tilmes, S., Tost, H., van Noije, T., van Zyl, P. G., von Salzen, K., Yu, F., Wang, Z., Wang, Z., Zaveri, R. A., Zhang, H., Zhang, K., Zhang, Q., and Zhang, X.: The AeroCom evaluation and intercomparison of organic aerosol in global models, Atmos. Chem. Phys., 14, 10845-10895, https://doi.org/10.5194/acp-14-10845-2014, 2014.

Vereecken, L. and Nozière, B.: H migration in peroxy radicals under atmospheric conditions, Atmos. Chem. Phys., 20, 7429-7458, https://doi.org/10.5194/acp-20-7429-2020, 2020.

Vereecken, L. and Peeters, J.: A structure–activity relationship for the rate coefficient of H-migration in substituted alkoxy radicals, Phys. Chem. Chem. Phys., 12, 12608-12620, https://doi.org/10.1039/C0CP00387E 2010.

Vereecken, L., Müller, J.-F., and Peeters, J.: Low-volatility poly-oxygenates in the OH-initiated atmospheric oxidation of α-pinene: impact of non-traditional peroxyl radical chemistry, Phys. Chem. Chem. Phys., 9, 5241-5248, https://doi.org/10.1039/b708023a, 2007.

Vereecken, L., Aumont, B., Barnes, I., Bozzelli, J. W., Goldman, M. J., Green, W. H., Madronich, S., Mcgillen, M. R., Mellouki, A., Orlando, J. J., Picquet-Varrault, B., Rickard, A. R., Stockwell, W. R., Wallington, T. J., and Carter, W. P. L.: Perspective on mechanism development and structure-activity relationships for gas-phase atmospheric chemistry, International journal of chemical kinetics, 50, 435-469, https://doi.org/10.1002/kin.21172, 2018.

Wang, H., Shen, H., Zhao, D., Kang, S., Wu, R., Baker, Y., He, Q., Zanders, A., Bachner, M., Worsnop, D. R., Hohaus, T., Mentel, T. F., and Zorn, S. R.: Exploring the Hydrogen Abstraction Pathway in HOM Formation from α-pinene Photooxidation Systems under Varying NO Conditions, EGUsphere [preprint], 2026, 1-24, https://doi.org/10.5194/egusphere-2026-1083, 2026.

Wang, Z., Ehn, M., Rissanen, M. P., Garmash, O., Quéléver, L., Xing, L., Monge-Palacios, M., Rantala, P., Donahue, N. M., Berndt, T., and Sarathy, S. M.: Efficient alkane oxidation under combustion engine and atmospheric conditions, Communications chemistry, 4, 18, https://doi.org/10.1038/s42004-020-00445-3, 2021.

Xu, L., Møller, K. H., Crounse, J. D., Otkjær, R. V., Kjaergaard, H. G., and Wennberg, P. O.: Unimolecular reactions of peroxy radicals formed in the oxidation of α-pinene and β-pinene by hydroxyl radicals, J. Phys. Chem. A, 123, 1661-1674, https://doi.org/10.1021/acs.jpca.8b11726, 2019.

Yang, L., Nie, W., Yan, C., Ehn, M., Liu, Y., Roldin, P., Qi, X., Kerminen, V.-M., Donahue, N. M., Worsnop, D., Kulmala, M., and Ding, A.: A mechanistic understanding of the varying yields of highly oxygenated organic molecules, Nature Communications, https://doi.org/10.1038/s41467-025-67007-w, 2025.

Ziemann, P. J. and Atkinson, R.: Kinetics, products, and mechanisms of secondary organic aerosol formation, Chem. Soc. Rev., 41, 6582-6605, https://doi.org/10.1039/C2CS35122F 2012.